OFFICE OF CIVILIAN RADIOACTIVE WASTE MANAGEMENT
ANALYSIS/MODEL COVER SHEET

1. QA: QA

Page: 1 of: 52

Complete Only Applicable Items

2. ☒ Analysis	Check all that apply
Type of Analysis	☐ Engineering ☒ Performance Assessment ☐ Scientific
Intended Use of Analysis	☐ Input to Calculation ☒ Input to another Analysis or Model ☐ Input to Technical Document ☐ Input to other Technical Products
Describe use: Provide input to waste package and drip shield degradation analysis.	

3. ☒ Model	Check all that apply
Type of Model	☐ Conceptual Model ☒ Abstraction Model ☐ Mathematical Model ☐ System Model ☐ Process Model
Intended Use of Model	☐ Input to Calculation ☒ Input to another Model or Analysis ☐ Input to Technical Document ☐ Input to other Technical Products
Describe use: Provide input to waste package and drip shield degradation analysis.	

4. Title:
Abstraction of Models of Stress Corrosion Cracking of Drip Shield and Waste Package Outer Barrier and Hydrogen Induced Corrosion of Drip Shield

5. Document Identifier (including Rev. No. and Change No., if applicable):
ANL-EBS-PA-000004 REV 00 ICN 01

6. Total Attachments:
3

7. Attachment Numbers - No. of Pages in Each:
I-3 pages, II-6 pages, III-6 pages

	Printed Name	Signature	Date
8. Originator	Kevin G. Mon Bryan E. Bullard	Kevin Mon Bryan Bullard	11/8/00 11/8/00
9. Checker	David Stahl	Pamparthi for David Stahl	11/8/00
10. Lead/Supervisor	Kevin G. Mon	Kevin Mon	11/8/00
11. Responsible Manager	Robert J. MacKinnon	R.J. MacKinnon for R.J. MacKinnon	11/8/00

12. Remarks:

Kevin Mon is responsible for the entire document.
Bryan Bullard is responsible for Section 6.2.

The results of the abstraction analyses documented in this AMR are tracked by DTN: MO0010MWDSUP04.010 (Stress Corrosion Cracking analyses results) and DTN: MO0010SPASUP04.011 (Manufacturing Defect Model analyses results).

For TSPA-SR.

Win-11 NM5507

OFFICE OF CIVILIAN RADIOACTIVE WASTE MANAGEMENT

ANALYSIS/MODEL REVISION RECORD

Complete Only Applicable Items

2. Analysis or Model Title:

Abstraction of Models of Stress Corrosion Cracking of Drip Shield and Waste Package Outer Barrier and Hydrogen Induced Corrosion of Drip Shield

3. Document Identifier (including Rev. No. and Change No., if applicable):

ANL-EBS-PA-000004 REV 00 ICN 01

4. Revision/Change No.	5. Description of Revision/Change
00	Initial Issue
00 ICN 01	Interim Change to incorporate changes due to the removal of backfill and new/revised upstream inputs. Reorganized discussion of models used/developed. Changes are indicated by vertical change bars on the right margin. Outer lid renamed to extended closure lid; inner lid renamed to flat closure lid

TABLE OF CONTENTS

Page

1. PURPOSE 8

2. QUALITY ASSURANCE 8

3. COMPUTER SOFTWARE AND MODEL USAGE 9
3.1 COMPUTER SOFTWARE 9
3.1.1 Mathcad 2000 Professional 9
3.2 MODELS USED 9
3.2.1 Stress Corrosion Cracking of the Drip Shield and the Waste Package Outer Barrier Process Model 9

4. INPUTS 10
4.1 DATA AND PARAMETERS 10
4.2 CRITERIA 14
4.2.1 Acceptance Criteria Applicable To All Six Sub-Issues 14
4.2.2 Acceptance Criteria For Sub-Issue 1 15
4.2.3 Acceptance Criteria for Sub-Issue 2 16
4.3 CODES AND STANDARDS 17

5. ASSUMPTIONS 17
5.1 TITANIUM GRADE 7 DRIP SHIELD STRESS CORROSION AND HYDROGEN INDUCED CRACKING 17
5.2 MANUFACTURING DEFECTS IN CLOSURE LID WELDS 18
5.3 STRESS AND STRESS INTENSITY FACTOR PROFILES IN CLOSURE LID WELDS 20
5.4 SLIP DISSOLUTION MODEL 21
5.5 THRESHOLD STRESS INTENSITY FACTOR (K_{ISCC}) MODEL 22

6. ANALYSIS/MODEL 22
6.1 STRESS CORROSION CRACKING AND HYDROGEN INDUCED CRACKING OF DRIP SHIELD 23
6.2 MANUFACTURING DEFECTS ABSTRACTION MODEL 24
6.2.1 Abstraction Methodology 24
6.2.2 Implementation of Closure Lid Weld Defect Flaw Abstraction Results in Waste Package Degradation Analysis 29
6.2.3 Manufacturing Defect Abstraction Model Validation 30
6.3 STRESS AND STRESS INTENSITY FACTOR PROFILE ABSTRACTION MODEL 30
6.3.1 Abstraction Methodology 30
6.3.2 Stress and Stress Intensity Factor Profile Abstraction Model Validation 40
6.4 SLIP DISSOLUTION ABSTRACTION MODEL 41
6.4.1 Abstraction Approach and Methodology 41
6.4.2 Crack Growth Rate 42

6.4.3 Threshold Stress for Crack Growth Initiation 43
6.4.4 Incipient Cracks and Manufacturing Defects 43
6.4.5 Slip Dissolution Model Analysis 44
6.4.6 Slip Dissolution Abstraction Model Validation 45
6.5 THRESHOLD STRESS INTENSITY FACTOR ABSTRACTION MODEL 45
6.5.1 Threshold Stress Intensity Factor Abstraction Model Validation 46

7. CONCLUSIONS 47

8. INPUTS AND REFERENCES 50
8.1 DOCUMENT CITED 50
8.2 CODES, STANDARDS, REGULATIONS, AND PROCEDURES 51
8.3 SOURCE DATA, LISTED BY DATA TRACKING NUMBER 52

9. ATTACHMENTS 52

LIST OF FIGURES

Page

Figure 1. The probability flaws are not detected as a function of b and v (25-mm extended closure lid weld) (Source: CRWMS M&O 2000c, Figure 1; DTN: MO0001SPASUP03.001). 26

Figure 2. Conditional probability density functions of defect flaw sizes in the closure lid welds for various combinations of values for parameters, b and v (Source: CRWMS M&O 2000c, Figure 2; DTN: MO0001SPASUP03.001). 27

Figure 3. Hoop stress as a function of depth in the extended closure lid welds (25-mm thick) at the reference location on the extended closure lid weld circumference and the uncertainty range 33

Figure 4. Stress intensity factor as a function of radial crack depth in the extended closure lid welds (25-mm thick) at the reference location on the extended closure lid weld circumference and the uncertainty range 34

Figure 5. Hoop stress as a function of depth in the extended closure lid welds (25-mm thick) at 0°, 90° and 180° angles along the circumference of the extended closure lid weld. 34

Figure 6. Stress intensity factor as a function of radial crack depth in the extended closure lid welds (25-mm thick) at 0°, 90° and 180° angles along the extended closure lid weld circumference. 35

Figure 7. Hoop stress as a function of the projected depth in the flat closure lid welds (10-mm thick) at the reference location on the flat closure lid weld circumference and the uncertainty range. 35

Figure 8. Stress intensity factor as a function of the projected radial crack depth in the flat closure lid welds (10-mm thick) at the reference location on the flat closure lid weld circumference and the uncertainty range 36

Figure 9. Hoop stress as a function of the projected depth in the flat closure lid welds (10-mm thick) at 0°, 90° and 180° angles along the circumference of the flat closure lid weld. 36

Figure 10. Stress intensity factor as a function of the projected radial crack depth in the flat closure lid welds (10-mm thick) at 0°, 90° and 180° angles along the flat closure lid weld circumference. 37

Figure 11. Hoop stress as a function of depth in the Alloy 22 extended closure lid welds (25-mm thick) at the reference location on the extended lid weld circumference using uncertainty bounds of ± 5, 10, and 30% 38

Figure 12. Stress intensity factor as a function of radial crack depth in the Alloy 22 extended closure lid welds (25-mm thick) at the reference location on the extended closure lid weld circumference using uncertainty bounds of ± 5, 10, and 30% 39

Figure 13. Hoop stress as a function of radial crack depth in the Alloy 22 flat closure lid welds (10-mm thick) at the reference location on the flat closure lid weld circumference using uncertainty bounds of ± 5, 10, and 30% 39

Figure 14. Stress intensity factor as a function of depth in the Alloy 22 flat closure lid welds (10-mm thick) at the reference location on the flat closure lid weld circumference using uncertainty bounds of ± 5, 10, and 30% 40

Figure 15. Bounding calculations for the model responses for the time to failure of the extended and flat closure lids by SCC calculated with the slip dissolution model using the bounding values for parameter *n* for a range of the stress intensity factor values 44

Figure 16. Probability density function of the threshold stress intensity factor of the waste package outer barrier closure lids (Alloy 22) 46

LIST OF TABLES

Page

Table 1. Data and Parameters and Their Sources. 10

Table 2. Stress Intensity Factor (K_I) vs. Depth Tables for the Extended and Flat Closure Lids of Waste Package Outer Barrier. 11

Table 3. Values of the Coefficients in Equation 1 for the Stress Profiles of the Extended and Flat Closure Lid Welds of the Waste Package Outer Barrier. 12

Table 4. Values of the Coefficients Used in Equation 1 for the Stress Profile of the Waste Package Outer Barrier Extended Closure Lid Welds from DTN: LL000316005924.140. 12

Table 5. Yield Strength (CRWMS M&O 1999c, Section 5.7) (see also Section 6.4.3) and Fraction of the Yield Strength for the Uncertainty of the Stress State in the Extended and Flat Closure Lid Welds of the Waste Package Outer Barrier (CRWMS M&O 2000a, Section 6.2.2). 13

Table 6. Percentages of Manufacturing Defect Flaws in Various Thickness Regions of Extended and Flat Closure Lid Welds of the Waste Package Outer Barrier. 14

Table 7. Coefficients of the Polynomial Equation to Calculate the Stress State versus Depth for the Extended and Flat Closure Lids (converted to metric units relative to those in Table 3). 31

Table 8. Figures to be compared between this AMR and the upstream process level AMR. 41

1. PURPOSE

As directed by a written development plan (CRWMS M&O 1999a), an analysis for the degradation of drip shield and waste package in the engineered barrier system (EBS) is conducted. The purpose of this analysis is to assist Performance Assessment Department (PAD) and its EBS Performance Section in analyzing process models of stress corrosion cracking (SCC) of waste package (CRWMS M&O 2000a) and hydrogen induced cracking (HIC) of drip shield (CRWMS M&O 2000d), and develop abstractions of the models, which are used as input to the WAste Package DEGradation (WAPDEG) model (CRWMS M&O 2000b). The WAPDEG model is used in the total system performance assessment (TSPA) for waste package and drip shield degradation analysis. The purpose of this document is to allow PAD to provide a more detailed and complete waste package and drip shield degradation abstraction and to answer the key technical issues (KTI) raised in the U.S. Nuclear Regulatory Commission (NRC) Issue Resolution Status Report (IRSR) for the Container Lifetime and Source Term (CLST) Revision 2 (NRC 1999). Comments by the TSPA Peer Review Panel (Budnitz, et al. 1999) were considered and none were applicable to the current analysis.

The abstracted models documented in this technical product are potentially important to the evaluation of principle factors for the post-closure safety case, particularly those related to performance of the drip shield and waste package barriers. Therefore, these abstraction models have primary (Level 1) importance. The scope of the current abstraction analysis is limited to the SCC and HIC processes (and their process models and parameters) that significantly affect the performance of waste packages and drip shields in the repository (CRWMS M&O 2000a). The processes that do not have significant impact on the drip shield and waste package performance are not considered. Also, the model abstractions documented in this AMR are based on the process models and their parameters documented in the associated AMR (CRWMS M&O 2000a). The abstraction analyses documented in this AMR are for the current potential repository design (CRWMS M&O 2000h). In this design, a drip shield is placed over the waste package and no backfill is emplaced over the drip shield (CRWMS M&O 2000h Section 2.5). The output from the abstraction analyses is intended to be used as input to the WAPDEG analysis for waste package and drip shield degradation.

Alternative approaches to representing the uncertainty and variability of the stress state and stress intensity factor in the closure lid welds of waste package are also evaluated.

2. QUALITY ASSURANCE

The Quality Assurance (QA) program applies to the development of this documentation for the abstraction analyses of stress corrosion cracking (SCC) of waste package outer barrier and drip shield and hydrogen induced cracking (HIC) of drip shield. The Performance Assessment Department responsible manager has evaluated the technical document development activity in accordance with QAP-2-0, *Conduct of Activities*. The QAP-2-0 activity evaluation, *Conduct of Performance Assessment* (CRWMS M&O 1999b), has determined that the preparation and review of this technical document is subject to *Quality Assurance Requirements and Description* (QARD) DOE/RW-0333P (DOE 2000) requirements. Preparation of this analysis did not

require the classification of items in accordance with QAP-2-3, *Classification of Permanent Items*. This activity is not a field activity. Therefore, an evaluation in accordance with NLP-2-0, *Determination of Importance Evaluations* was not required.

The methods used to control the electronic management of data as required by AP-SV.1Q, *Control of the Electronic Management of Information*, were not specified in the Development Plan, *Model Abstraction to Support WAPDEG Analysis of Waste Package and Drip Shield Degradation* (CRWMS M&O 1999a). With regard to the development of this AMR, the control of electronic management of data was evaluated in accordance with YAP-SV.1Q, *Control of the Electronic Management of Data*. The evaluation (CRWMS M&O 2000j) determined that current work processes and procedures are adequate for the control of electronic management of data for this activity. Though YAP-SV.1Q has been replaced by AP-SV.1Q, this evaluation remains in effect.

3. COMPUTER SOFTWARE AND MODEL USAGE

3.1 COMPUTER SOFTWARE

3.1.1 Mathcad 2000 Professional

Mathcad 2000 Professional is a commercially available software used in this analysis. This software, in accordance with AP-SI.1Q, *Software Management*, is appropriate for this application as it offers all of the mathematical and graphical functionality necessary to perform and document the numerical manipulations used in this analysis. Mathcad 2000 Professional was executed on a DELL PowerEdge 2200 Workstation equipped with two Pentium II 266 MHz processors (CRWMS M&O tag 112371) in the Windows NT 4.0 operating system. No macros were developed and only built-in functions were used, thus there is no need to conduct software validation exercises. Details of the Mathcad numerical manipulations performed are discussed where they are used in Attachments I through III of this analysis.

3.2 MODELS USED

3.2.1 Stress Corrosion Cracking of the Drip Shield and the Waste Package Outer Barrier Process Model

The Stress Corrosion Cracking of the Drip Shield and the Waste Package Outer Barrier Process Model is developed, documented, and validated in the Analyses and Models Report (AMR) entitled *Stress Corrosion Cracking of the Drip Shield, the Waste Package Outer Barrier and the Stainless Steel Structural Material* (CRWMS M&O 2000a). This model is appropriate for its intended use in this analysis. This model was not implemented in code in the AMR and no TDMS Model Warehouse DTN was obtained.

4. INPUTS

4.1 DATA AND PARAMETERS

Data and parameters that are input to this analysis include stress and stress intensity profiles (stress or stress intensity versus depth), threshold stress, incipient crack densities, and crack growth rate model and model parameters appropriate for both the outer shell extended and outer shell flat closure lids of the waste package outer barrier (CRWMS M&O 2000h, Figure 2-13). In this analysis, the outer shell extended closure lid shall be referred to simply as the extended closure lid and the outer shell flat closure lid shall be referred to as the flat closure lid. These data were acquired or developed under quality assurance procedures. Table 1 summarizes these data, their sources, data tracking numbers (DTNs), and other associated information.

Table 1. Data and Parameters and Their Sources.

Parameter	Source	DTN	Where Documented in this Document
Stress Intensity Factor Profiles of WP Closure Lid Welds	CRWMS M&O 2000a Sections 6.2.2.4 & 6.2.2.5 Attachment I	LL000316005924.140 LL000316105924.141	Table 2
Coefficients for Stress Profile Equation of WP Closure Lid Welds	CRWMS M&O 2000a Sections 6.2.2.2 Attachment I	LL000316005924.140 LL000316105924.141	Table 3
Yield Strength of Alloy 22 at 125 °C	CRWMS M&O 1999c Section 5.7	MO0003RIB00071.000[a]	Table 5
Various Fractions of Yield Strength to account for Uncertainty of Stress and Stress Intensity Factor of WP Closure Lid Welds	CRWMS M&O 2000a Section 6.2.2.5	N/A	Table 5
Threshold Stress Intensity Factor	CRWMS M&O 2000a Section 6.3.2	N/A	Section 6.5
Threshold Stress	CRWMS M&O 2000a Section 6.5.2	N/A	Section 6.4.3
Incipient Crack Density	CRWMS M&O 2000a Section 6.5.2	N/A	Section 6.4.4
Slip Dissolution Model and Model Parameters	CRWMS M&O 2000a Section 6.4 Equations 22 to 24	N/A	Equations 2 to 4 Section 4.1 Section 6.4.2
Probability of Manufacturing Defect Flaws in Waste Package Closure Lid Welds	CRWMS M&O 2000g Section 6.2.1 CRWMS M&O 2000i Section 6.2.1, Attachment III	N/A	Table 6 Section 6.2

[a] DTN obtained from RIB database.

DTN: LL000316005924.140 and DTN: LL000316105924.141 are qualified data.

Table 2. Stress Intensity Factor (K_I) vs. Depth Tables for the Extended and Flat Closure Lids of Waste Package Outer Barrier.

Extended Closure Lid		Flat Closure Lid	
KI ($MPa \cdot m^{1/2}$)	Depth (mm)	KI ($MPa \cdot m^{1/2}$)	Depth (mm)
-8.096912553	0.3988	-7.201806034	0.3277
-11.08864448	0.8001	-10.05117186	0.6579
-13.12743778	1.1989	-12.14661052	0.9855
-14.62395207	1.6002	-13.83718048	1.3132
-15.74125563	1.9990	-15.26051182	1.6408
-16.56494834	2.4003	-16.48813922	1.971
-17.16634511	2.7991	-17.60873931	2.2987
-17.5702798	3.2004	-18.62418012	2.6264
-17.79521296	3.5992	-19.34568044	2.954
-17.85960516	3.9980	-18.27353932	3.2842
-17.77785124	4.3993	-17.05876838	3.6119
-17.56148906	4.7981	-15.73543176	3.9395
-17.22755067	5.1994	-14.40693057	4.2697
-16.78515648	5.5982	-13.09502192	4.5974
-16.23441637	5.9995	-11.74410433	4.9251
-15.58159374	6.3983	-10.37129779	5.2527
-14.83251247	6.7970	-8.992063026	5.5829
-13.99233711	7.1984	-7.619959749	5.9106
-13.06249616	7.5971	-6.28349195	6.2382
-12.03771518	7.9985	-5.021547684	6.5659
-10.93137807	8.3972	-3.791766552	6.8961
-9.747286832	8.7986	-2.602642611	7.2238
-8.489320377	9.1973	-1.461856773	7.5514
-7.161148843	9.5987	-0.376262524	7.8791
-5.7664094	9.9974	0.6479086	8.2093
-4.327309665	10.3962	1.602739435	8.5369
-2.830795383	10.7975	2.489890331	8.8646
-1.280437794	11.1963	3.304704392	9.1948
0.320255595	11.5976	4.043027992	9.5225
1.967753102	11.9964	4.701256926	9.8501
3.658542826	12.3977	5.276226526	10.1778
5.415098304	12.7965	5.809253288	10.508
7.218783158	13.1978	6.267459831	10.8356
9.05768593	13.5966	6.633989902	11.1633
10.92825736	13.9954	6.907239191	11.491
12.82690422	14.3967	7.086141819	11.8212
14.74987947	14.7955	7.170016506	12.1488
16.73175271	15.1968	7.171796631	12.4765
18.7698867	15.5956	7.082153019	12.8067
20.82285508	15.9969	6.8851964	13.1343
22.88648224	16.3957	6.581695963	13.462
24.95692222	16.7945	6.173014275	13.7897
27.03021919	17.1958	5.661052333	14.1199
29.13461342	17.5946	5.214086954	14.4475
31.33328838	17.9959	5.185517036	14.7752
33.52559005	18.3947	5.092620849	15.1028
35.70701317	18.7960	4.940639873	15.433
37.87294261	19.1948	4.735255128	15.7607
40.01865333	19.5961	4.482741007	16.0884
42.13953021	19.9949	4.18995429	16.4186

Note:The extended closure lid data is from p. A-29, Attachment I, CRWMS M&O 2000a (also DTN: LL000316005924.140). The flat closure lid data is from p. A-46, Attachment I, CRWMS M&O 2000a (also DTN: LL000316105924.141).

Stress State

Stress (σ_s in ksi) as a function of depth (x in inches) in the closure lid welds of the waste package outer barrier is given by a third order polynomial equation of the form (CRWMS M&O 2000a, Section 6.2.2):

$$\sigma_s(x) = A_0 + A_1 \cdot x + A_2 \cdot x^2 + A_3 \cdot x^3 \qquad \text{(Eq. 1)}$$

where the values of the coefficients (A_i's) used in this analysis are given in Table 3.

Table 3. Values of the Coefficients in Equation 1 for the Stress Profiles of the Extended and Flat Closure Lid Welds of the Waste Package Outer Barrier.

Coefficient	Extended Closure Lid	Flat Closure Lid
A_0	-51.672275	-63.486
A_1	136.97241	651.94
A_2	134.40677	-1460.30
A_3	-155.15755	872.50

Note: The stress determined in Equation 1 through the use of these coefficients is in ksi.

The flat closure lid coefficients are from the Excel File S&K_IL_Peen (DTN: LL000316105924.141).

The extended lid coefficients listed in Table 3 are not exactly the same as those reported in Revision 00 of this document and submitted to the TDMS (Excel File S&K_OL_Anne (DTN: LL000316005924.140)) as shown in Table 4.

Table 4. Values of the Coefficients Used in Equation 1 for the Stress Profile of the Waste Package Outer Barrier Extended Closure Lid Welds from DTN: LL000316005924.140.

Coefficient	Extended Closure Lid
A_0	-51.6776
A_1	137
A_2	134.367
A_3	-155.147

Note: The stress determined in Equation 1 through the use of these coefficients is in ksi.

The differences between the values in Table 3 and Table 4 have no significant impact on the results of this analysis as shown in Attachment I.

Stress State Uncertainty

The uncertainty in the stress state of the extended and flat closure lid welds is calculated using the yield strength (YS) and fraction of the yield strength of the lid materials (Alloy 22) as discussed in Section 6.3. The data are given in Table 5.

Table 5. Yield Strength (CRWMS M&O 1999c, Section 5.7) (see also Section 6.4.3) and Fraction of the Yield Strength for the Uncertainty of the Stress State in the Extended and Flat Closure Lid Welds of the Waste Package Outer Barrier (CRWMS M&O 2000a, Section 6.2.2).

Parameter	Value
Yield Strength (*YS*) at 125 °C	46.72 ksi
Fraction of Yield Strength Used for Uncertainty in Stress and Stress Intensity Factor Profiles	5% - Optimum 10% - Realistic 30% - Conservative

Stress State Variability

The variability of the mean stress along the circumference of the extended or flat closure lids is represented with a sinusoidal variation with a range of 5 ksi about the mean stress (CRWMS M&O 2000a, Section 6.2.2).

Slip Dissolution Model for Crack Initiation and Growth

Once crack growth initiates the crack(s) grow at a velocity given by (CRWMS M&O 2000a, Section 6.4.4):

$$V_t = \overline{A}(K_I)^{\overline{n}} \quad \text{(Eq. 2)}$$

where V is the crack growth rate in mm/s, and K_I is the stress intensity factor in MPa·m$^{1/2}$. Parameters, $\overline{A}$ and $\overline{n}$, in the above equation are expressed as follows (CRWMS M&O 2000a, Section 6.4.4).

$$\overline{A} = 7.8x10^{-2}\, n^{3.6}\left(4.1x10^{-14}\right)^n \quad \text{(Eq. 3)}$$

$$\overline{n} = 4n \quad \text{(Eq. 4)}$$

The uncertainty in the model parameter n is represented by a uniform distribution with an upper bound of 0.84 and a lower bound of 0.75 (CRWMS M&O 2000a, Section 6.4.4).

From the recently obtained longer-term data, the model parameter n and its uncertainty have been re-evaluated. n is represented by a uniform distribution with an upper bound of 0.92 and a lower bound of 0.843 (CRWMS M&O 2000a, Section 6.4.4).

Manufacturing Defect Flaw Percentages

In Attachment III of the upstream AMR, *Analysis of Mechanisms for Early Waste Package Failure* (CRWMS M&O 2000i, Attachment III), values are provided for the percentage manufacturing defect flaws embedded in the outer ¼ of the weld thickness and which are surface breaking. These values are presented in Table 6 along with their sums.

Table 6. Percentages of Manufacturing Defect Flaws in Various Thickness Regions of Extended and Flat Closure Lid Welds of the Waste Package Outer Barrier.

Description from CRWMS M&O 2000i, Attachment III	Embedded in Outer ¼ of Thickness	Outer Surface Breaking	Sum
Case 5, 1inch, SS, MMA, RT&PT, Shop	34.32%	0.49%	34.81%
Case 1, 1inch, SS, MMA, RT&PT	35.77%	0.40%	36.17%
Case 3, 2.5 inch, SS, MMA, RT&PT	36.19%	0.13%	36.32%

The sum of the percentages can be used to account for the possibility that embedded flaws can become surface breaking due to general corrosion processes (see Assumption 5.2.1).

4.2 CRITERIA

The Nuclear Regulatory Commission (NRC) Issue Resolution Status Report (IRSR) on Container Lifetime and Source Term (NRC 1999) is used as criteria for this analysis. Specific acceptance criteria used are the general acceptance criteria and those applicable to Subissues 1 and 2. Listed below are the six Subissues from the Container Lifetime and Source Term IRSR:

(1) The effects of corrosion processes on the lifetime of the containers (NRC 1999, Section 2.2).

(2) The effects of phase instability of materials and initial defects on the mechanical failure and lifetime of the containers (NRC 1999, Section 2.2).

(3) The rate at which radionuclides in spent nuclear fuel (SNF) are released from the Engineered Barrier System (EBS) through the oxidation and dissolution of spent fuel (NRC 1999, Section 2.2).

(4) The rate at which radionuclides in high-level waste (HLW) glass are leached and released from the EBS (NRC 1999, Section 2.2).

(5) The effect of in-package criticality on waste package (WP) and EBS performance (NRC 1999, Section 2.2).

(6) The effects of alternate EBS design features on container lifetime and radionuclide release from the EBS (NRC 1999, Section 2.2).

Of these sub-issues, only sub-issues (1) and (2) are relevant to this analysis.

4.2.1 Acceptance Criteria Applicable To All Six Sub-Issues

(1) The collection and documentation of data, as well as development and documentation of analyses, methods, models, and codes, are accomplished under approved quality assurance and control procedures and standards (NRC 1999, Section 4.0).

(2) Expert elicitations, when used, are conducted and documented in accordance with the guidance provided in NUREG-1563 (Kotra, et. al., 1996) or other acceptable approaches (NRC 1999, Section 4.0).

(3) Sufficient data (field, laboratory, and natural analog) are obtained to adequately define relevant parameters for the models used to evaluate performance aspects of the sub-issues (NRC 1999, Section 4.0).

(4) Sensitivity and uncertainty analyses (including consideration of alternative conceptual models) are used to determine whether additional data would be needed to better define ranges of input parameters (NRC 1999, Section 4.0).

(5) Parameter values, assumed ranges, test data, probability distributions, and bounding assumptions used in the models are technically defensible and can reasonably account for known uncertainties (NRC 1999, Section 4.0).

(6) Mathematical model limitations and uncertainties in modeling are defined and documented (NRC 1999, Section 4.0).

(7) Primary and alternative modeling approaches consistent with available data and current scientific understanding are investigated and their results and limitations considered in evaluating the sub-issue (NRC 1999, Section 4.0).

(8) Model outputs are validated through comparisons with outputs of detailed process models, empirical observations, or both (NRC 1999, Section 4.0).

(9) The structure and organization of process and abstracted models adequately incorporate important design features, physical phenomena, and coupled processes (NRC 1999, Section 4.0).

4.2.2 Acceptance Criteria For Sub-Issue 1

(1) Identify and consider likely modes of corrosion for container materials, including dry-air oxidation, humid-air corrosion, and aqueous corrosion processes, such as general corrosion, localized corrosion, microbial-induced corrosion (MIC), stress corrosion cracking (SCC), and hydrogen embrittlement, as well as the effect of galvanic coupling (NRC 1999, Section 4.1.1).

(2) Identify the broad range of environmental conditions within the WP emplacement drifts that may promote the corrosion processes listed previously, taking into account the possibility of irregular wet and dry cycles that may enhance the rate of container degradation (NRC 1999, Section 4.1.1).

(3) Demonstrate that the numerical corrosion models used are adequate representations, taking into consideration associated uncertainties, of the expected long-term behaviors and are not likely to underestimate the actual degradation of the containers as a result of corrosion in the repository environment (NRC 1999, Section 4.1.1).

(4) Consider the compatibility of container materials, the range of material conditions, and the variability in container fabrication processes, including welding, in assessing the performance expected in the container's intended waste isolation function (NRC 1999, Section 4.1.1).

(5) Justify the use of data collected in corrosion tests not specifically designed or performed for the Yucca Mountain repository program for the environmental conditions expected to prevail at the Yucca Mountain site (NRC 1999, Section 4.1.1).

(6) Conduct a consistent, sufficient, and suitable corrosion testing program at the time of the LA submittal. In addition, DOE shall identify specific plans for further testing to reduce any significant area(s) of uncertainty as part of the performance confirmation program (NRC 1999, Section 4.1.1).

(7) Establish a defensible program of corrosion monitoring and testing of the engineered subsystems components during the performance confirmation period to assure they are functioning as intended and anticipated (NRC 1999, Section 4.1.1).

4.2.3 Acceptance Criteria for Sub-Issue 2

(1) Identify and consider the relevant mechanical failure processes that may affect the performance of the proposed container materials (NRC 1999, Section 4.2.1).

(2) Identify and consider the effect of material stability on mechanical failure processes for the various container materials as a result of prolonged exposure to the expected range of temperatures and stresses, including the effects of chemical composition, microstructure, thermal treatments, and fabrication processes (NRC 1999, Section 4.2.1).

(3) Demonstrate that the numerical models used for container materials stability and mechanical failures are effective representations, taking into consideration associated uncertainties, of the expected materials behavior and are not likely to underestimate the actual rate of failure in the repository environment (NRC 1999, Section 4.2.1).

(4) Consider the compatibility of container materials and the variability in container manufacturing processes, including welding, in its WP failure analyses and in the evaluation of radionuclide release (NRC 1999, Section 4.2.1).

(5) Identify the most appropriate methods for nondestructive examination of fabricated containers to detect and evaluate fabrication defects in general and, particularly, in seam and closure welds (NRC 1999, Section 4.2.1).

(6) Justify the use of material test results not specifically designed or performed for the Yucca Mountain repository program for environmental conditions (i.e., temperature, stress, and time) expected to prevail at the proposed Yucca Mountain repository (NRC 1999, Section 4.2.1).

(7) Conduct a consistent, sufficient, and suitable materials testing program at the time of the License Application submittal. In addition, DOE has identified specific plans for further testing to reduce any significant area(s) of uncertainty as part of the performance confirmation program (NRC 1999, Section 4.2.1).

(8) Establish a defensible program of monitoring and mechanical testing of the engineered subsystems components, during the performance confirmation period, to assure they are functioning as intended and anticipated, in the presence of thermal and stress perturbations (NRC 1999, Section 4.2.1).

4.3 CODES AND STANDARDS

No codes and standards are used in this analysis.

5. ASSUMPTIONS

The following assumptions were made. All of the assumptions document accepted scientific practice and are consistent with assumptions made in the supporting AMRs. None of the following assumptions require any further confirmation in addition to the bases provided below prior to the use of the parameters developed in this document.

5.1 TITANIUM GRADE 7 DRIP SHIELD STRESS CORROSION AND HYDROGEN INDUCED CRACKING

5.1.1 It is assumed that the only source of stress (necessary for stress corrosion cracking (SCC)) in the drip shield is the loading due to rockfall. The assumption is based on an assumption listed in the upstream Analysis and Models Report (AMR) (CRWMS M&O 2000a, Section 5, Assumption 1). In this AMR, it is stated that stresses due to seismic activity will not induce SCC because these stresses are temporary in nature. It is also stated that weld residual stress, normally a major source of SCC, will be eliminated from the welds in the DS by an annealing process. This assumption is used throughout this analysis. This assumption does not need to be verified since it is reasonable and consistent with the current state of scientific knowledge.

5.1.2 Although SCC of the Ti Grade 7 drip shield is possible, it is of low consequence to drip shield performance and is therefore not modeled. Cracks in passive alloys, such as Ti Grade 7, tend to be very tight (i.e., small crack opening displacement) by nature (CRWMS M&O 2000a, Section 6.5.5). The opposing sides of through-wall cracks will continue to corrode at very low passive corrosion rates until the gap region of the tight crack opening is "plugged" by the corrosion product particles and mineral precipitates such as carbonate present in the water. Any water transport through this oxide/salt filled crack area will be mainly by diffusion-type transport processes (CRWMS M&O 2000a, Section 6.5.5). Thus, the effective water flow rate through cracks in the drip shield would be expected to be extremely low and should not contribute significantly to the overall radionuclide release rate from the underlying failed waste package. Therefore, since the primary role of the drip shield is to keep water from contacting the waste package, SCC and HIC of the drip shield is of low consequence. This assumption is used

throughout this analysis. This assumption does not need to be verified since it is reasonable and consistent with the current state of scientific knowledge.

5.2 MANUFACTURING DEFECTS IN CLOSURE LID WELDS

Assumptions used to develop the abstraction for the probability and size of manufacturing defects in the Alloy 22 waste package outer barrier extended and flat closure lid welds are described in detail in the abstraction calculation (CRWMS M&O 2000c, Section 5). The major assumptions that are important to the effect of the manufacturing defects on SCC are listed below.

5.2.1 Surface breaking defects are considered, since these are the types of flaws that may potentially lead to stress corrosion cracking (SCC). Note that there is uncertainty associated with this assumption because, as general corrosion propagates, some of the pre-existing surface-breaking defects may disappear, and embedded defects would become surface-breaking defects. This uncertainty could be accounted for through the use of model parameters based on the sum of the percentages of surface breaking and flaws embedded in the outer ¼ of the weld surfaces (CRWMS M&O 2000a, Section 6.5.1) (see Table 6 and associated comments). This assumption is used in the abstraction analysis of manufacturing defects in waste package closure lid welds in Section 6.2. This assumption does not need to be verified since it is reasonable and consistent with the current state of scientific knowledge.

5.2.2 Flaws are assumed to be spatially randomly distributed as represented by a Poisson process (CRWMS M&O 2000c, Section 3). If the characteristics of flaw occurrence in the welds are consistent with the following five (Poisson process) properties, then the assumption is reasonable.

- There are no flaws at zero weld length. This amounts to an initial condition for the model.
- The numbers of flaws that occur in non-overlapping lengths of weld metal are independent.
- The distribution of the number of flaws depends only on the length of weld metal considered.
- For small weld segments, the probability of a flaw is proportional to the length of the weld. This constant of proportionality is denoted by λ.
- There are no simultaneous flaws, meaning that the probability of obtaining two or more flaws in a sufficiently small segment of weld is negligible.

These assumptions are reasonable for the manufacturing processes being considered. This assumption is used in the abstraction analysis of manufacturing defects in the Alloy 22 waste package outer barrier closure lid welds in Section 6.2. This assumption does not need to be verified since it is reasonable and consistent with the current state of scientific knowledge.

5.2.3 The mean flaw density (Poisson distribution parameter) of the closure weld is assumed to be 0.6839 flaws per meter of one inch thick weld as given in the process model analysis (CRWMS M&O 2000i, Section 6.2.1). This is a reasonable value based on the literature reviewed for the process model analysis (CRWMS M&O 2000i, Section 8). This assumption is used in the abstraction analysis of manufacturing defects in the Alloy 22 waste package outer barrier closure lid welds in Section 6.2. This assumption does not need to be verified since it is reasonable and consistent with the current state of scientific knowledge.

5.2.4 The fraction of surface breaking flaws is assumed to be uniformly distributed between the minimum and maximum fractions (0.13% and 0.49%) used to determine the average fraction quoted in the process model analysis (CRWMS M&O 2000a, Section 6.5.1). The basis of this assumption is that the three values (0.13%, 0.40% and 0.49%) quoted in the process model analysis are not sufficient to determine a single representative average value (CRWMS M&O 2000c, Section 3). The use of the uniform distribution is a reasonable representation of the uncertainty in expressing this value. This assumption is used in the abstraction analysis of manufacturing defects in the Alloy 22 waste package outer barrier closure lid welds in Section 6.2. This assumption does not need to be verified since it is reasonable and consistent with the current state of scientific knowledge.

5.2.5 It is assumed that cases 1, 3, and 5 from Attachment III of the upstream AMR, *Analysis of Mechanisms for Early Waste Package Failure* (CRWMS M&O 2000i, Attachment III) are appropriate to derive the fraction of flaws considered capable of propagation in the Alloy 22 waste package extended and flat closure lid welds (see Table 6). The basis of this assumption is that these cases are considered adequate for representing the highly controlled environment under which the welding will be performed. This assumption is used in the abstraction analysis of manufacturing defects in the Alloy 22 waste package outer barrier closure lid welds in Section 6.2. This assumption does not need to be verified since it is reasonable and consistent with the current state of scientific knowledge.

5.2.6 The sum of the fractions of surface breaking flaws and flaws embedded in the outer ¼ of the weld surfaces (the fraction of flaws considered capable of propagation) is assumed to be uniformly distributed between the minimum and maximum fractions (34.81% and 36.32%) (see Table 6). The basis of this assumption, like the previous one, is that the three values (34.81%, 36.17%, and 36.32%) quoted in Table 6 are not sufficient to determine a single representative average value (CRWMS M&O 2000c, Section 3). The use of the uniform distribution is a reasonable representation of the uncertainty in expressing this value. This assumption is used in the abstraction analysis of manufacturing defects in the Alloy 22 waste package outer barrier closure lid welds in Section 6.2. This assumption does not need to be verified since it is reasonable and consistent with the current state of scientific knowledge.

5.2.7 Pre-inspection flaw sizes are assumed to be lognormally distributed, with distribution parameters (dependent on the weld thickness) as given in the process model analysis (CRWMS M&O 2000g, Section 6.2.1 and CRWMS M&O 2000i, Section 6.2.1). The assumption is employed because it provided the best fit to the flaw size data used in the

upstream process model analysis (CRWMS M&O 2000g, Section 6.2.1 and CRWMS M&O 2000i, Section 6.2.1). This assumption is used in the abstraction analysis of manufacturing defects in the Alloy 22 waste package outer barrier closure lid welds in Section 6.2. This assumption does not need to be verified since it is reasonable and consistent with the current state of scientific knowledge.

5.2.8 The probability of non-detection is given as a function of flaw size as discussed in the process model analysis (CRWMS M&O 2000i, Section 6.2.1). The model is dependent on the following parameters: the detection threshold (p), the location parameter (b), and a scale parameter (v). The b and v parameters are taken to be uncertain with a uniform distribution. This is a reasonable assumption, as the manufacturing and detection processes for welds on the waste container are not specified to date. The values are based on similar industrial manufacturing practices as reviewed in the process model analysis. The basis for this assumption should be checked as data is developed on actual welds. This assumption is used in the abstraction analysis of manufacturing defects in the Alloy 22 waste package outer barrier closure lid welds in Section 6.2. This assumption does not need to be verified since it is reasonable and consistent with the current state of scientific knowledge.

5.2.9 It is assumed that all detrimental flaws detected are repaired to specified acceptance criteria or removed in such a manner that they are eliminated from consideration for further failure analysis. This assumption is based on a similar assumption in the *Analysis of Mechanisms for Early Waste Package Failure* AMR (CRWMS M&O 2000i, Assumption 5.3). This assumption is used in the abstraction analysis of manufacturing defects in the Alloy 22 waste package outer barrier closure lid welds in Section 6.2. This assumption does not need to be verified since it is reasonable and consistent with the current state of scientific knowledge.

5.3 STRESS AND STRESS INTENSITY FACTOR PROFILES IN CLOSURE LID WELDS

The following assumptions were used to develop abstractions for stress and stress intensity factor profiles in the closure lid welds (extended and flat closure lids) of the outer barrier of waste package.

5.3.1 It is assumed that all fabrication welds of waste package, except the welds for closure lids, are fully annealed before the waste packages are loaded with waste and not subject to SCC (CRWMS M&O 2000a, Section 5, Assumption 1). This assumption is used in the abstraction analysis of stress and stress intensity factor profiles in the Alloy 22 waste package outer barrier closure lid welds in Section 6.3. This assumption does not need to be verified since it is reasonable and consistent with the current state of scientific knowledge.

5.3.2 The hoop stress (and the corresponding stress intensity factor for radial cracks) is the prevailing stress in the closure lid welds that fail the waste packages by SCC if it occurs. Thus, the current abstraction is limited to the profiles for the hoop stress and corresponding stress intensity factor for radial cracks (CRWMS M&O 2000a, Section 6.5.1). This assumption is used in the abstraction analysis of stress and stress intensity

factor profiles in the Alloy 22 waste package outer barrier closure lid welds in Section 6.3. This assumption does not need to be verified since it is reasonable and consistent with the current state of scientific knowledge.

5.3.3 The hoop stress and corresponding stress intensity factor profiles in the flat closure lid welds from the process model analysis are for a plane that is inclined at about 37.5° from a plane normal to the outer surface of the flat closure lid (CRWMS M&O 2000a, Figure AI-1). Because the SCC analysis in the integrated waste package degradation model (WAPDEG) assumes that cracks propagate in the direction normal to the lid surface, the profiles from the process model analysis were projected to the plane normal to the outer surface of the lid. The SCC analysis with the projected profiles properly represents the hoop stress and stress intensity factor profiles for the inclined plane. This assumption is used in the abstraction analysis of stress and stress intensity factor profiles in the Alloy 22 waste package outer barrier closure lid welds in Section 6.3. This assumption does not need to be verified since it is reasonable and consistent with the current state of scientific knowledge.

5.3.4 The hoop stress and corresponding stress intensity factor profiles versus depth in the closure lid welds from the process model analyses represent the mean profiles (CRWMS M&O 2000a, Attachment I). The uncertainties in the hoop stress and corresponding stress intensity factor profiles are represented with triangular distributions around the mean profiles (CRWMS M&O 2000a, Section 6.2.2.5). This assumption is used in the abstraction analysis of stress and stress intensity factor profiles in the Alloy 22 waste package outer barrier closure lid welds in Section 6.3. This assumption does not need to be verified since it is reasonable and consistent with the current state of scientific knowledge.

5.3.5 The hoop stress and stress intensity factor profiles vary along the circumference of the closure lid welds, and this represents the variability in the profiles on a given waste package. The same degree of the profile variability is applied equally to all the waste packages in the repository, and there is no variability in the profiles among waste packages. This assumption is used in the abstraction analysis of stress and stress intensity factor profiles in the Alloy 22 waste package outer barrier closure lid welds in Section 6.3. This assumption does not need to be verified since it is reasonable and consistent with the current state of scientific knowledge.

5.3.6 As a crack propagates in the closure lid welds or the welds corrode by corrosion, stresses in the welds may re-distribute in such a way to mitigate the SCC initiation and crack growth (CRWMS M&O 2000a, Section 6.2.2). Such stress re-distribution or relaxation is not considered in the current abstraction. This assumption is used in the abstraction analysis of stress and stress intensity factor profiles in the Alloy 22 waste package outer barrier closure lid welds in Section 6.3. This is a conservative bounding condition such that additional confirmation is not needed.

5.4 SLIP DISSOLUTION MODEL

The following assumptions were used to develop abstraction for the slip dissolution model for the SCC crack growth.

5.4.1 Induction-heating solution annealing is used to mitigate residual stress in the extended closure lid welds, and laser peening in the flat closure lid welds (CRWMS M&O 2000a, Section 6.2.2.4). The process-model manufacturing defect analyses (CRWMS M&O 2000g, Section 6.2.1 and CRWMS M&O 2000i, Section 6.2.1) and the abstraction calculation (CRWMS M&O 2000c, Section 5) are assumed applicable to the closure lid welds after the stress annealing processes. This assumption is used in the abstraction analysis of the Slip Dissolution Model and model parameters in Section 6.4. This assumption does not need to be verified since it is reasonable and consistent with the current state of scientific knowledge.

5.4.2 It is assumed that the analyses for incipient cracks reported in the process model analysis (CRWMS M&O 2000a, Section 6.5.2) are applicable to the closure lid welds after the stress mitigation process. This assumption is used in the abstraction analysis of the Slip Dissolution Model and model parameters in Section 6.4. This assumption does not need to be verified since it is reasonable and consistent with the current state of scientific knowledge.

5.5 THRESHOLD STRESS INTENSITY FACTOR (K_{ISCC}) MODEL

The following assumption was employed in the SCC analysis with the threshold stress intensity factor (K_{ISCC}) model.

5.5.1 As recommended in the process model analysis (CRWMS M&O 2000a, Section 6.3.1), the threshold stress intensity factor (K_{ISCC}) model is applied to pre-existing flaws such as manufacturing defects in the closure lid welds. This assumption is used in the abstraction analysis of the Threshold Stress Intensity Factor Model and model parameters in Section 6.5. The effect of different exposure conditions (including applied stress) on the K_{ISCC} value, and improved characterization of its uncertainty and variability under those varying exposure conditions will be made as additional data and analysis are developed (CRWMS M&O 2000a, Section 6.3.2). This assumption does not need to be verified since it is reasonable and consistent with the current state of scientific knowledge.

6. ANALYSIS/MODEL

This section documents analyses to develop abstractions for models and parameters for stress corrosion cracking (SCC) of waste package and drip shield and hydrogen induced cracking (HIC) of drip shield. As discussed in Section 6.1 below, SCC and HIC of drip shield would not affect the drip shield performance under the repository conditions. No further analysis was conducted for model abstraction of SCC and HIC of the drip shield. The results of the abstraction analyses documented in this AMR are tracked by DTN: MO0010MWDSUP04.010 (Stress Corrosion Cracking analyses results) and DTN: MO0010SPASUP04.011 (Manufacturing Defect Model analyses results).

In order for SCC to occur, three factors must be present: metallurgical susceptibility, a critical environment, and a static (or sustained) tensile stress (CRWMS M&O 2000a, Section 6.1). Except for the Alloy 22 waste package outer barrier extended and flat closure lid welds, all the fabrication welds in the waste packages are assumed fully annealed and not subject to SCC.

Also, the major sources of stresses in the drip shield induced by earthquakes are insignificant to SCC (CRWMS M&O 2000a, Section 5, Assumption 1). Therefore, the abstractions for the SCC model discussed in this section are for the extended and flat closure lid welds in the waste package outer barrier. The current abstraction analysis does not address detailed potential effects of microstructure-scale processes on SCC such as dislocation, aging, noble element enrichment, etc.

In the current waste package degradation analysis, two alternative SCC models, the Slip Dissolution (or Film Rupture) Abstraction Model and the Threshold Stress Intensity Factor (K_{ISCC}) Abstraction Model, are considered (CRWMS M&O 2000a, Section 3.2). In the Threshold Stress Intensity Factor Abstraction Model, the threshold stress intensity factor (K_{ISCC}) is used to determine when SCC will occur. Provided that an initial flaw and corrosive environment is present, a SCC failure will occur when the applied stress intensity factor K_I is greater than or equal to the threshold stress intensity factor K_{ISCC} (i.e., $K_I \geq K_{ISCC}$). The Slip Dissolution Abstraction Model assumes that incipient cracks or defects grow continuously when the oxidation reaction that occurs at the crack tip ruptures the protective film via an applied strain in the underlying matrix. The rate at which the crack grows is a function of the crack tip strain, environmental conditions, and material properties. The theory and fundamentals of the SCC models are described in detail in the process model analysis (CRWMS M&O 2000a, Sections 6.3 and 6.4). This section documents the model abstractions for the two alternative SCC models.

6.1 STRESS CORROSION CRACKING AND HYDROGEN INDUCED CRACKING OF DRIP SHIELD

As discussed in the process model analysis report (CRWMS M&O 2000a, Assumption 1), the drip shield is assumed to be fully stress-relief annealed before it is placed in the emplacement drift. As discussed in Section 5.1, the only source of stress in the drip shield (necessary for stress corrosion cracking to occur) is the loading due to rockfall. If SCC of the drip shield occurs it will result in the formation of cracks. The cracks will become plugged with corrosion products and/or other mineral precipitates (see Assumption 5.1.2) leading to very little water transport. Therefore, SCC of the drip shield does not significantly compromise the intended function of the drip shield (i.e., water diversion) and thus is of low consequence to drip shield performance. No additional analysis was conducted for SCC of drip shield.

Hydrogen induced cracking (HIC) of drip shield is a potential degradation mechanism that could cause failure of drip shield if the hydrogen uptake in the titanium drip shield is greater than the critical hydrogen concentration (1,000 μg/g) (CRWMS M&O 2000d, Section 5). In addition to the hydrogen concentration being greater than the threshold concentration, stress is required to cause hydrogen induced cracking in the drip shield. Crevice corrosion and passive general corrosion of the drip shield are two feasible processes in the repository that could lead to hydrogen absorption by the drip shield. Hydrogen is produced as a result of the corrosion processes. In a drip shield design without backfill, hydrogen generation could also result from galvanic couples formed between the drip shield and structural components (such as rock bolts, wire mesh, and steel drift liners), which may fall on the drip shield surface. Some of the hydrogen produced can be absorbed by the titanium metal and then transported into the metal by diffusion. Because the drip shield will not be subject to crevice corrosion under the exposure conditions anticipated in the repository (CRWMS M&O 2000d, Section 6.1.4), general corrosion and galvanic couple formation are the only mechanisms that could cause HIC in the drip shield.

Results of the bounding analyses of the general corrosion process have shown that the time that the hydrogen uptake concentration reaches the critical hydrogen concentration under the exposure conditions anticipated in the repository is greater than 10,000 years (CRWMS M&O 2000d, Section 6.2.3) . Therefore it is concluded that HIC due to the general corrosion process is not a limiting degradation process.

Galvanic couples formed between the drip shield and steel structural components are likely to have a small contact area and a low anode (the steel structural component) to cathode (the larger drip shield) area ratio (CRWMS M&O 2000d, Section 6.3.2). This coupled with the relatively low volumes of water likely to contact both materials simultaneously, leads to the conclusion that the effects of such galvanic couples should be local in effect and short lived in duration. The conditions in the repository will be oxidizing, making it unlikely that the couple will sustain water reduction and hence hydrogen absorption. Furthermore, as noted above, the hydrogen concentration must reach relatively high levels in Ti Grade 7 before HIC can occur (CRWMS M&O 2000d, Section 6.3.2). Lastly, even if HIC did occur on the drip shield (due to general corrosion or galvanic couple formation) and resulted in through-wall cracks, the crack openings will be plugged by corrosion products and/or other mineral precipitates (see Assumption 5.1.2) leading to very little water transport through the drip shield. Therefore HIC is of little consequence to drip shield performance. For these reasons, no additional analysis of HIC of the drip shield was conducted.

6.2 MANUFACTURING DEFECTS ABSTRACTION MODEL

This model abstraction is used to calculate the probability of the occurrence and size of manufacturing defects in the Alloy 22 waste package outer barrier closure lid welds. Assumptions associated with this model are discussed in Section 5.2. The Manufacturing Defects Abstraction Model documented in this technical product is potentially important to the evaluation of principle factors for the post-closure safety case, particularly those related to performance of the drip shield and waste package barriers. Therefore, this abstraction model has primary (Level 1) importance. Many of the data and parameters used in this model are also documented in the calculation entitled *Calculation of Probability and Size of Defect Flaws in Waste Package Closure Welds to Support WAPDEG Analysis* (CRWMS M&O 2000c) and are tracked by DTN: MO0001SPASUP03.001. The analysis presented in the above calculation was based on inputs derived from the Analyses and Models Report (AMR) *Analysis of Mechanisms for Early Waste Package Failure* (CRWMS M&O 2000g). In the present analysis, the functional forms and parameters used in the model are updated to reflect recent changes in the *Analysis of Mechanisms for Early Waste Package Failure* AMR (CRWMS M&O 2000i).

6.2.1 Abstraction Methodology

Calculation of the flaw depth distribution begins with the initial (pre-inspection) flaw size distribution. This distribution is assumed lognormal with the probability density function is given by

$$f(s) = \frac{1}{s\sigma\sqrt{2\pi}} exp\left[-\frac{1}{2\sigma^2}\left(ln\frac{s}{a_{50}}\right)^2\right] \qquad s > 0 \qquad \text{(Eq. 5)}$$

where s is the flaw size. The probability density function in Equation 5 is the derivative of the cumulative probability density ($F(a)$) as given in CRWMS M&O 2000i, Section 6.2.1. The parameters, a_{50} and σ, are given as functions of weld thickness (t, in millimeters) (CRWMS M&O 2000i, Section 6.2.1),

$$a_{50}(t) = 0.1169 \cdot 25.4 - 0.0445 \cdot t + \frac{0.00797}{25.4} \cdot t^2 \quad \text{(Eq. 6)}$$

$$\sigma(t) = 0.09733 + \frac{0.3425}{25.4} \cdot t - \frac{0.07268}{(25.4)^2} \cdot t^2 \quad \text{(Eq. 7)}$$

Here a_{50} is the median or geometric mean of the distribution and σ is the standard deviation of the natural log transformed flaw sizes ($ln(s)$ values). For a 10-mm weld thickness, a_{50} is equal to 2.556 and σ is equal to 0.221. For a 25-mm weld thickness, a_{50} is equal to 2.053 and σ is equal to 0.364.

Note that in a previous version of the source AMR (CRWMS M&O 2000g, Section 6.2.1), the median and standard deviation were given (t, in millimeters) by,

$$a_{50}(t) = 0.1159 \cdot 25.4 - 0.0445 \cdot t + \frac{0.00797}{25.4} \cdot t^2 \quad \text{(Eq. 8)}$$

$$\sigma(t) = 0.09733 + \frac{0.3425}{25.4} \cdot t - \frac{0.07288}{(25.4)^2} \cdot t^2 \quad \text{(Eq. 9)}$$

The small changes in the third significant digits of the first coefficient of $a_{50}(t)$ and the third coefficient in $\sigma(t)$ have little effect on the results of any analysis. For a 10-mm weld thickness, a_{50} is equal to 2.530 and σ is equal to 0.221. For a 25-mm weld thickness, a_{50} is equal to 2.027 and σ is equal to 0.364.

Next, the post-inspection flaw size distribution must be derived. The final closure weld is subject to a multi-angular ultrasonic exam (UT) where the probability of non-detection (PND) is given as a function of flaw size, s, (CRWMS M&O 2000i, Section 6.2.1 see also Assumption 5.5)

$$PND(s) = \left[p + 0.5 \cdot (1-p) \cdot erfc\left(v \cdot ln\left(\frac{s}{b} \right) \right) \right]^2 = \left[\frac{p+1}{2} + \frac{p-1}{2} \cdot erf\left(v \cdot ln\left(\frac{s}{b} \right) \right) \right]^2 \quad \text{(Eq. 10)}$$

Here p is the lower limit of PND (0.005), erf is the error function, b is the location parameter, and v is the scale parameter. The *Early Waste Package Failure* AMR (CRWMS M&O 2000i, Section 6.2.1) states that the PND for various size defects is dependent on a number of variables such as the type of material, operator skill, access to the weld, and type of defect. As these types of factors cannot be determined at this point in time the parameters, b and v will be taken to be uncertain. Values elicited from the literature for b range from 2.5 to 5 mm (CRWMS M&O 2000i, Figure 4) (note that 1.6 to 5 mm have been used previously (CRWMS M&O 2000c, Section 6)). Values for v range from 1 to 3 (CRWMS M&O 2000c, Section 6).

The probability that a flaw is not detected (let B be the set of flaws not detected) is then the definite integral from zero to the thickness of the weld:

$$Pr(B \mid b,\nu) = \int_0^t PND(s) \cdot f(s) \cdot ds \qquad \text{(Eq. 11)}$$

These probabilities for a 25-mm thick closure weld for various values for b and ν are shown in Figure 1.

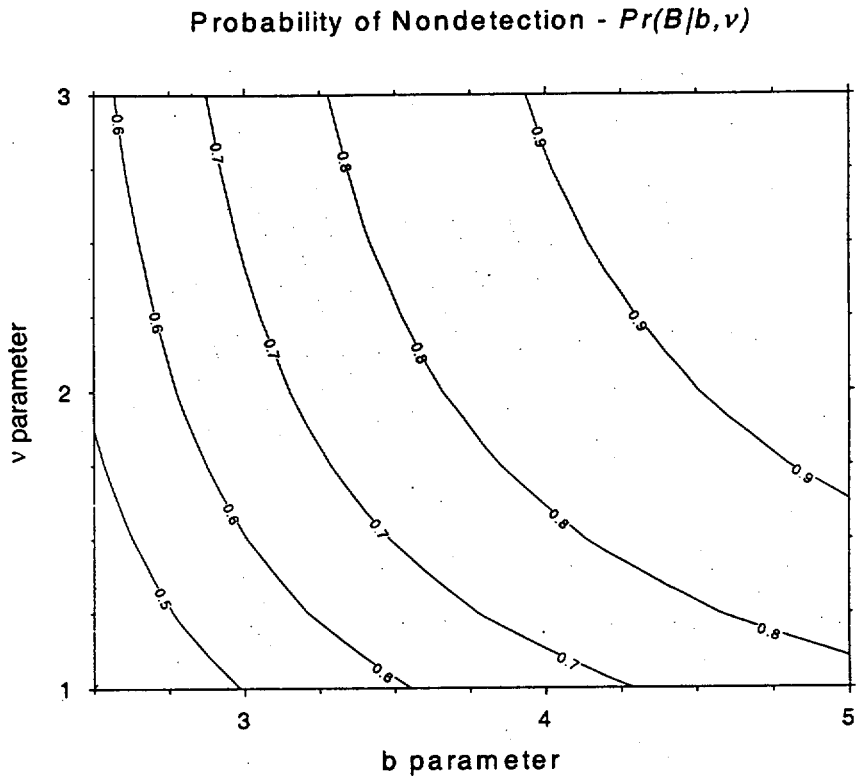

Figure 1. The probability flaws are not detected as a function of b and ν (25-mm extended closure lid weld) (Source: CRWMS M&O 2000c, Figure 1; DTN: MO0001SPASUP03.001).

The conditional probability density function (pdf) for flaw size, s, (given that the flaw is not detected) is then:

$$g(s \mid b,\nu) = \frac{PND(s) \cdot f(s)}{Pr(B \mid b,\nu)} \qquad \text{(Eq. 12)}$$

Figure 2 shows several pdfs for a 25-mm thick closure weld for various combinations of values for b and ν.

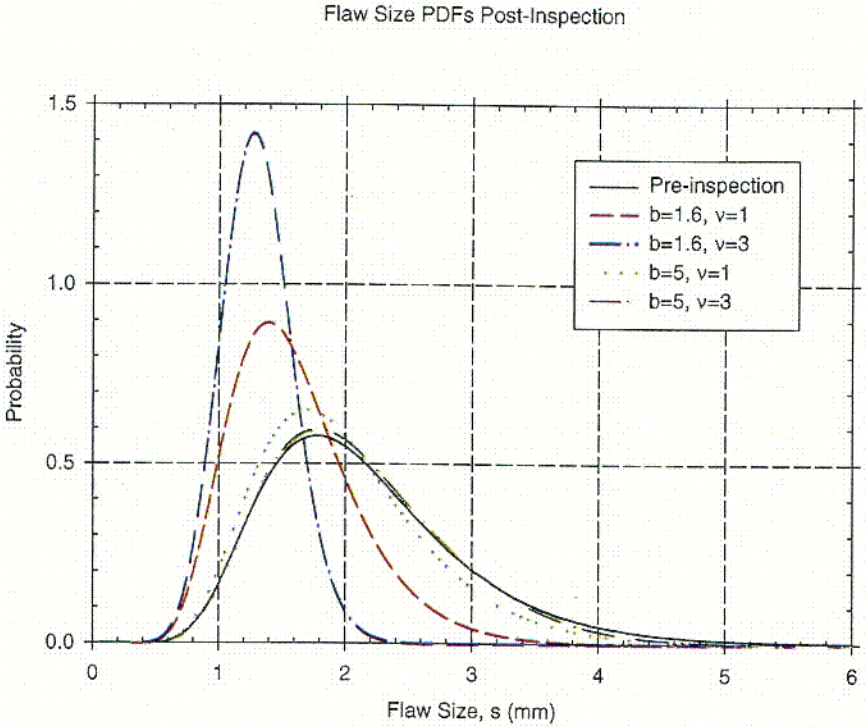

Figure 2. Conditional probability density functions of defect flaw sizes in the closure lid welds for various combinations of values for parameters, *b* and *v* (Source: CRWMS M&O 2000c, Figure 2; DTN: MO0001SPASUP03.001).

With cumulative distribution function given as,

$$G(s \mid b,v) = \frac{\int_0^s PND(x) \cdot f(x) \cdot dx}{Pr(B \mid b,v)} \qquad \text{(Eq. 13)}$$

Calculation of the outer surface-breaking mean flaw density begins with the base mean flaw density of $0.6839 \cdot 10^{-3}$ flaws/mm of weld for a one inch thick stainless steel Manual Metal Arc weld (this density was measured from an actual weld performed under shop conditions) subject to radiographic (RT) and dye-penetrant (PT) tests (CRWMS M&O 2000i, Section 6.2.1). To convert this value to a flaw density for an uninspected weld, the base flaw density is increased by the sum of the flaw reduction factors provided for the RT and PT tests. The adjustment for the RT exam increases the total flaw density by a factor of 12.8 while the PT exam, which detects only surface-breaking flaws, increases the density of only the surface-breaking flaws by a factor of 31.4 (CRWMS M&O 2000i, Section 6.2.1). More generally the mean flaw density per millimeter of weld is,

$$\lambda = 0.6839 \times 10^{-3} \cdot [1 + F_{os}(31.4 - 1)] \cdot 12.8 \qquad \text{(Eq. 14)}$$

C01

where F_{OS} is the fraction outer surface flaws. Note that previously this was given as,

$$\lambda = 0.6839 \times 10^{-3} \cdot [12.8 + 31.4 \cdot F_{OS}] \quad \text{(Eq. 15)}$$

(CRWMS M&O 2000c, Section 5).

Next the effect of weld thickness on flaw density is used to adjust for the actual weld thickness on the closure weld. The weld thickness factor $R(t)$ is given by

$$R(t) = \begin{cases} \dfrac{-1090[t/127]+205}{112}, & for \quad 6.35\,mm \le t \le 12.70\,mm \\ \dfrac{-640[t/127]+160}{112}, & for \quad 12.70\,mm \le t \le 19.05\,mm \\ \dfrac{960[t/127]-80}{112}, & for \quad 19.05\,mm \le t \le 25.40\,mm \\ \dfrac{2050[t/127]-186}{224}, & for \quad 25.40\,mm \le t \le 38.10\,mm \\ \dfrac{3390[t/127]-588}{224}, & for \quad 38.10\,mm \le t \le 50.80\,mm \\ \dfrac{8705[t/127]-2714}{224}, & for \quad 50.80\,mm \le t \end{cases} \quad \text{(Eq. 16)}$$

where t is the weld thickness (in millimeters) (CRWMS M&O 2000i, Figure 3). For the 10-mm thick closure weld, the weld thickness factor (R) is about 106.4%. For the 25-mm thick closure weld, the weld thickness factor (R) is about 97.3%.

Multiplying $\lambda \cdot R(t)$ by the circumference of the closure weld results in the flaw density per closure weld. A final multiplication by the fraction of considered (for orientation or depth position in the weld) flaws (ψ) results in the final mean flaw density of considered flaws per closure weld (λ).

$$\lambda = 0.6839 \times 10^{-3} \cdot [1 + F_{OS}(31.4 - 1)] \cdot 12.8 \cdot R(t) \cdot (2\pi r) \cdot \psi \quad \text{(Eq. 17)}$$

Here F_{OS} is the fraction outer surface flaws, $R(t)$ is the weld thickness factor with t being the weld thickness in millimeters, r is the radius of the closure lid in millimeters and ψ is the fraction of considered flaws.

A final adjustment for the probability for flaws detected by the UT exam gives a final expression for flaw density per closure weld.

$$\lambda(t, r, F_{OS}, b, v, \psi) = 0.6839 \times 10^{-3} \cdot [1 + F_{OS}(31.4 - 1)] \cdot 12.8 \cdot R(t) \cdot (2\pi r) \cdot \psi \cdot Pr(B \mid b, v) \quad \text{(Eq. 18)}$$

This result is a function of weld thickness, t, closure weld radius, r, fraction of outer surface flaws, F_{OS}, PND location parameter, b, PND scale parameter, v, and the fraction of considered flaws ψ. F_{OS} is given by a uniform distribution between 0.0013 and 0.0049 (see Table 6), b is

given by a uniform distribution between 2.5 and 5-mm, v is given by a uniform distribution between 1 and 3, and ψ is given by a uniform distribution between 0.3481 and 0.3632 (see Table 6).

For modeling purposes, this average density of flaws needs to be translated into a count of the number of flaws expected to occur in closure welds from package to package. This distribution of flaw occurrences on the closure welds of the waste package is modeled as a Poisson process (see Assumption 5.2.2).

The mean flaw density of a closure weld, λ, is the average value of the number of flaws per closure weld observed over many such welds. The probability distribution for the number of flaws, X, i.e., the Poisson distribution for the number of flaws (CRWMS M&O 2000c, Section 5) is given by the probability function

$$P(X = x) = \frac{(\lambda)^x}{x!} exp(-\lambda) \quad \text{(Eq. 19)}$$

The probability of occurrence of one or more flaws on a closure weld follows from this as

$$P(X \geq 1) = 1 - P(X = 0) = 1 - exp(-\lambda) \quad \text{(Eq. 20)}$$

6.2.2 Implementation of Closure Lid Weld Defect Flaw Abstraction Results in Waste Package Degradation Analysis

The number of flaws that appear on a patch is sampled stochastically as a Poisson random variable (see Assumption 5.2.2). For each flaw that occurs (i.e., when the number of flaws is not equal to zero), a flaw size is randomly assigned to it by sampling from the calculated flaw size cumulative distribution function (Figure 2). This flaw (with sampled location and size) is then used in the SCC analysis. The abstracted results are then input to the integrated waste package degradation model (WAPDEG) to analyze its effect on waste package performance (CRWMS M&O 2000b, Section 6.3.11).

The main activity undertaken in this abstraction is to assign uncertainty distributions to the parameters used in the variability models for the Alloy 22 waste package outer barrier extended and flat closure lid weld flaws. The instances of where uncertainty is included are for the parameters of 1) the flaw detection distribution (b and v), and 2) the fraction of flaws considered (ψ). The parameters are treated as follows. The b and v parameters of the detection distribution are allowed to uniformly range between 1.6 to 5 mm and 1 to 3, respectively (CRWMS M&O 2000c, Section 6). Recent changes in the upstream AMR *Analysis of Mechanisms for Early Waste Package Failure* (CRWMS M&O 2000i, Figure 4) indicate that b should be sampled from a uniform distribution between 2.5 and 5 mm. The fraction of flaws considered (ψ) in the upstream process model analysis (CRWMS M&O 2000g, Section 6.2.1) is an average of three observations (average (0.49%, 0.40%, 0.13%) = 0.34%). Instead of using a single value (i.e., 0.34%), it is allowed to uniformly range from 0.13% to 0.49% (CRWMS M&O 2000c, Section 3). An alternative distribution for (ψ), based on the sum of the fractions of surface breaking flaws and flaws embedded in the outer ¼ of the weld surface, would be a uniform range from 34.81% to 36.32% (see Table 6). No other changes in model parameters are necessary to account

for this larger percentage of flaws. The model parameters are varied independently. Sensitivity analyses with the proposed distributions of the parameters need to be conducted to analyze the affect of not knowing the correct (deterministic) value of the parameters.

6.2.3 Manufacturing Defect Abstraction Model Validation

The Manufacturing Defect Abstraction Model (MDAM) is an abstraction model. The validation method used in this section is to review the model parameters for reasonableness, or consistency in explanation of all relevant data. This results in an appropriate level of confidence in the MDAM to consider it validated. As the MDAM is an abstraction model, the only data relevant to this validation exercise are the engineering analyses being abstracted (CRWMS M&O 2000g, Section 6.2.1 and CRWMS M&O 2000i, Section 6.2.1). Note that the MDAM uses the same model parameters and functional forms as its parent engineering analyses. Therefore, the MDAM model parameters and functional forms are technical product output developed using qualified methods per AP-3.10Q. The fact that the functional forms and model parameters used in the MDAM are identical to those provided in the engineering analyses is considered sufficient to validate the model inputs (i.e., the abstracted models are consistent with the engineering analyses). Therefore, the MDAM inputs are validated and the model's functional forms are validated. This results in an appropriate level of confidence in the MDAM to consider it validated.

6.3 STRESS AND STRESS INTENSITY FACTOR PROFILE ABSTRACTION MODEL

This model abstraction is to calculate the stress state and stress intensity factor versus depth and their uncertainty and variability in the closure lid welds of waste package. The Stress and Stress Intensity Factor Profile Abstraction Model documented in this technical product is potentially important to the evaluation of principle factors for the post-closure safety case, particularly those related to performance of the drip shield and waste package barriers. Therefore, this abstraction model has primary (Level 1) importance. Assumptions associated with this model are discussed in Section 5.3.

6.3.1 Abstraction Methodology

The hoop stress (and the corresponding stress intensity factor for radial cracks) is the prevailing stress in the closure lid welds that fail the waste packages by SCC if it occurs (CRWMS M&O 2000a, Section 6.5.1). Thus, the current abstraction is limited to the profiles for the hoop stress and corresponding stress intensity factor for radial cracks.

The extended closure lid of the waste package outer barrier is 25-mm thick and composed of Alloy 22. The flat closure lid of the outer barrier is 10-mm thick and composed of Alloy 22. Details of the abstraction and analysis process are presented in Attachments II and III. The coefficients for the polynomial equation to calculate the stress versus depth (given in Table 3) were first converted from English units (i.e., ksi and inches) to metric units (i.e., MPa and millimeters). The resulting coefficients are shown in Table 7.

Table 7. Coefficients of the Polynomial Equation to Calculate the Stress State versus Depth for the Extended and Flat Closure Lids (converted to metric units relative to those in Table 3).

Coefficient	Extended Closure Lid	Flat Closure Lid
A_0	-356.26778	-437.720543
A_1	37.180767	176.967239
A_2	1.436391	-15.606072
A_3	-0.065282	0.367099

The provided hoop stress state was determined to vary with angle (θ) around the circumference of the waste package closure lid welds ($\theta = 0$ for a reference point arbitrarily chosen) according to the following functional form (CRWMS M&O 2000a, Section 6.2.2.5):

$$\sigma_t = \sigma_s(x) - (2.5 \cdot 6.894757) \cdot (1 - \cos(\theta)) \quad \text{(Eq. 21)}$$

Note that σ_s (defined in Equation 1) should use the stress coefficients (A_i) defined in Table 7 with x in units of millimeters, and *6.894757* is a conversion factor between ksi and MPa. Based on the angular stress variation in Equation 21, the stress intensity (K_I) variation with angle is given by

$$K_t(x,\theta) = K_s(x) \cdot \left(\frac{\sigma_t(Thck,\theta)}{\sigma_t(Thck,0)} \right) \quad \text{(Eq. 22)}$$

where *Thck* is the lid thickness (CRWMS M&O 2000a, Section 6.2.2.5) and $K_s(x)$ is one of the stress intensity profiles presented in Table 2.

Two alternative uncertainty models are considered in this analysis. Both uncertainty models make use of an uncertainty scaling factor, *sz(z)*, (in MPa) given by

$$sz(z) = \left(\frac{z \cdot YS \cdot F}{3} \right) \quad \text{(Eq. 23)}$$

where z represents the uncertainty variation away from the median value and is sampled randomly from a given distribution type. This uncertainty scaling factor is also a function of the yield strength (*YS*) and yield strength scaling factor (*F*).

In Uncertainty Model 1, the stress at a given depth, x, angle, θ, and uncertainty variation, z, is given by

$$\sigma(x,\theta,z) = \sigma_t(x,\theta) \frac{\sigma_t(Thck,\theta) + sz(z)}{\sigma_t(Thck,\theta)} \quad \text{(Eq. 24)}$$

and the stress intensity by

$$K(x,\theta,z) = K_t(x,\theta)\frac{\sigma_t(Thck,\theta)+sz(z)}{\sigma_t(Thck,\theta)} = K_s(x)\frac{\sigma_t(Thck,\theta)+sz(z)}{\sigma_t(Thck,0)} \quad \text{(Eq. 25)}$$

In Uncertainty Model 2, the stress relation is given by

$$\sigma(x,\theta,z) = \sigma_t(x,\theta)+sz(z) \quad \text{(Eq. 26)}$$

and the stress intensity factor relation is given by

$$K(x,\theta,z) = K_s(x)\frac{\sigma_t(Thck,\theta)}{\sigma_t(Thck,0)} + 0.058534\cdot sz(z)\cdot\sqrt{\pi\cdot x} \quad \text{(Eq. 27)}$$

The elicited radial crack path for the extended closure lid (driven by the hoop stress) is in a direction normal to the outer surface (CRWMS M&O 2000a, Figure 4), thus, the crack length corresponds to the crack depth for the extended closure lid. However, the elicited crack path for the flat closure lid is at an angle to the normal of the lid surface (CRWMS M&O 2000a, p. I-60 and I-61), and the depth of the crack with respect to the surface is determined by projecting the crack length onto the lid surface normal. The angle of projection (about 37.5 degrees) was estimated from the length of the hoop stress plane and the thickness of the flat closure lid (see CRWMS M&O 2000a, Figure I-1). Thus the *sine* of the angle (0.60887312121) multiplied by the crack length results in the crack depth with respect to the flat closure lid surface (i.e., in a direction normal to the flat closure lid outer surface).

6.3.1.1 Abstraction Results and Discussion of Uncertainty Model 1

The abstraction results for the uncertainty range (using Uncertainty Model 1) of the hoop stress at the weld centerline plane as a function of depth in the extended closure lid welds (25-mm thick) are given in Figure 3. The figures discussed in this section result from analyses presented in Attachments II and III using 0.30 for the fraction of yield strength (F) and assuming (see Assumption 5.3.4) z is given by a triangular distribution. The stress profiles in Figure 3 are at a reference location ($0°$ angle) on the circumference of the lid welds. As will be shown later (Figure 5), the reference location on the lid weld circumference was selected in such a way that it has the largest hoop stress. The figure shows that the hoop stress in the extended closure lid welds is compressive at the surface (from stress mitigation with the induction-heating solution annealing technique) and becomes tensile at a depth of about 8 mm. The uncertainty range becomes larger with the weld depth. The corresponding stress intensity factor profiles (using Uncertainty Model 1) as a function of radial crack depth are shown in Figure 4. The stress intensity factor is negative at the surface, consistent with the compressive stress at the surface shown in Figure 3, and becomes positive at a depth of about 12-mm. Therefore no SCC crack will initiate until the 12-mm thick layer is removed. As with the hoop stress, the uncertainty range of the stress intensity factor increases with the weld depth. Figure 5 and Figure 6 show respectively the hoop stress as a function of depth and the corresponding stress intensity factor as a function of radial crack depth, both at $0°$, $90°$, and $180°$ angle along the circumference of the extended closure lid welds. The reference location designated at 0° angle has the largest hoop

stress, and the location at *180°* angle has the least hoop stress. As shown in the figures, the variability of the both profiles along the weld circumference is minor.

The abstraction results for the uncertainty range (using Uncertainty Model 1) of the hoop stress as a function of the projected depth for the flat closure lid welds (10-mm thick) are given in Figure 7. The stress profiles are at a reference location (*0°* angle) on the circumference of the lid welds. The hoop stress in the flat closure lid welds is compressive at the surface (from stress mitigation with the laser peening technique), transits to tensile state at a projected depth of about 2-mm, and then back to compressive state at a projected depth of about 8.5-mm. The corresponding stress intensity factor profiles (using Uncertainty Model 1) as a function of the projected radial crack depth are shown in Figure 8. The stress intensity factor is negative at the surface and becomes positive at a projected depth of about 5-mm. Therefore no SCC crack will initiate until the (projected) 5-mm thick layer is removed. The uncertainty of the stress intensity factor increases slightly with the weld depth beyond the depth at which it becomes positive. Figure 9 and Figure 10 show respectively the hoop stress as a function of the projected depth and the corresponding stress intensity factor as a function of the projected radial crack depth, both at *0°*, *90°*, and *180°* angle along the circumference of the flat closure lid welds. As for the extended lid welds, the variability of the both profiles along the weld circumference of the flat closure lid is minor.

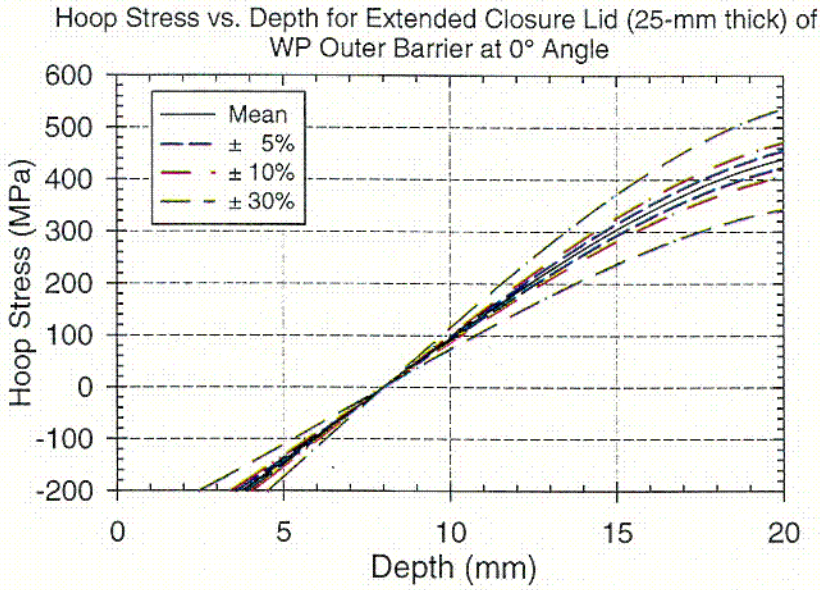

Figure 3. Hoop stress as a function of depth in the extended closure lid welds (25-mm thick) at the reference location on the extended closure lid weld circumference and the uncertainty range.

C02

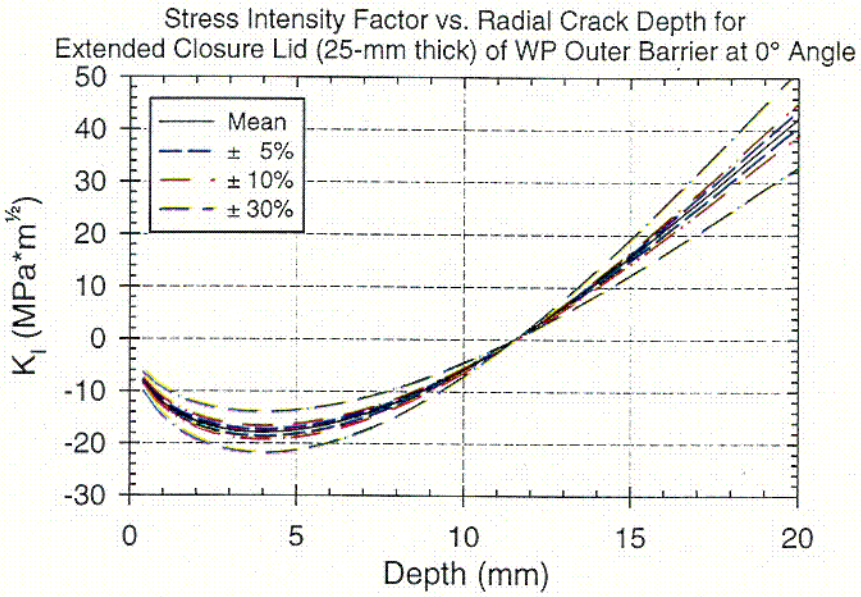

Figure 4. Stress intensity factor as a function of radial crack depth in the extended closure lid welds (25-mm thick) at the reference location on the extended closure lid weld circumference and the uncertainty range.

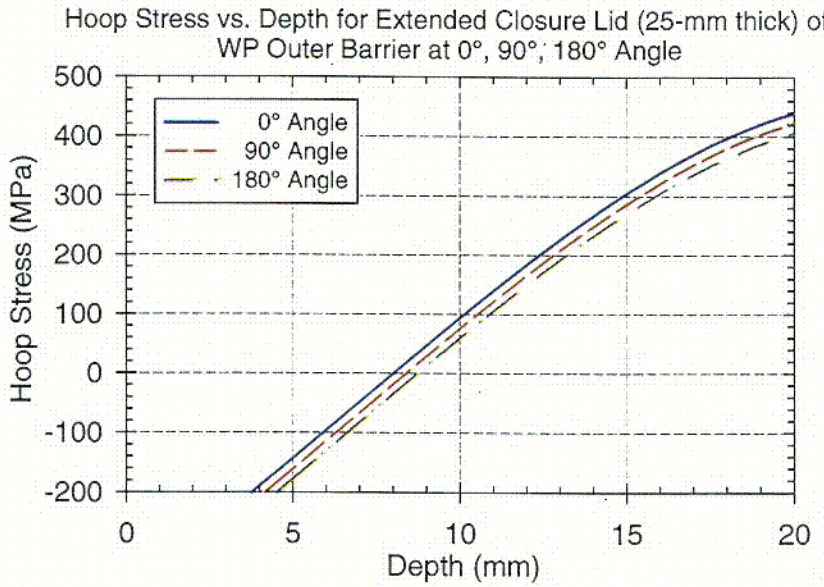

Figure 5. Hoop stress as a function of depth in the extended closure lid welds (25-mm thick) at 0°, 90° and 180° angles along the circumference of the extended closure lid weld.

C03

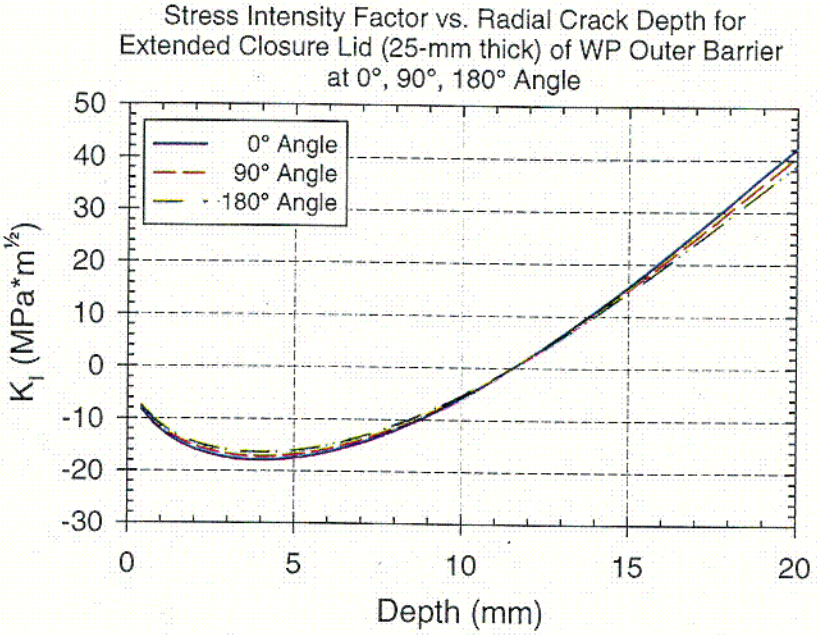

Figure 6. Stress intensity factor as a function of radial crack depth in the extended closure lid welds (25-mm thick) at 0°, 90° and 180° angles along the extended closure lid weld circumference.

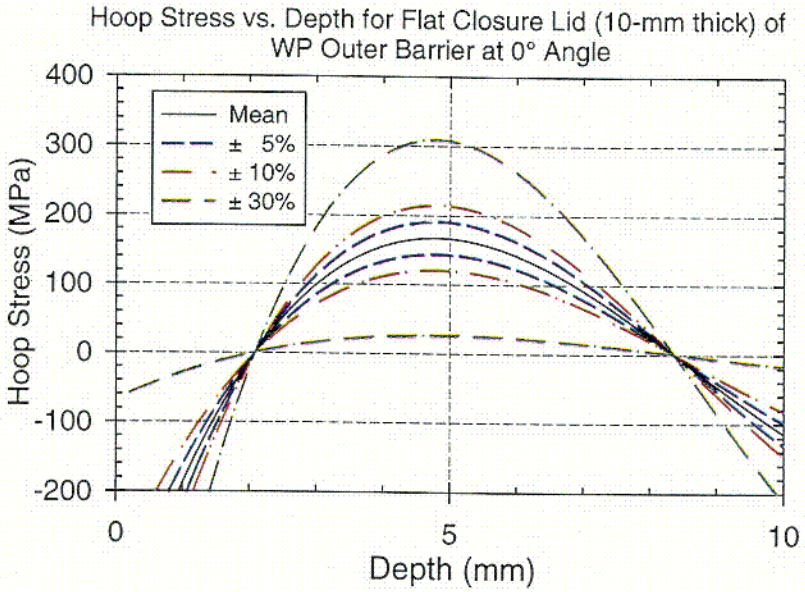

Figure 7. Hoop stress as a function of the projected depth in the flat closure lid welds (10-mm thick) at the reference location on the flat closure lid weld circumference and the uncertainty range.

C04

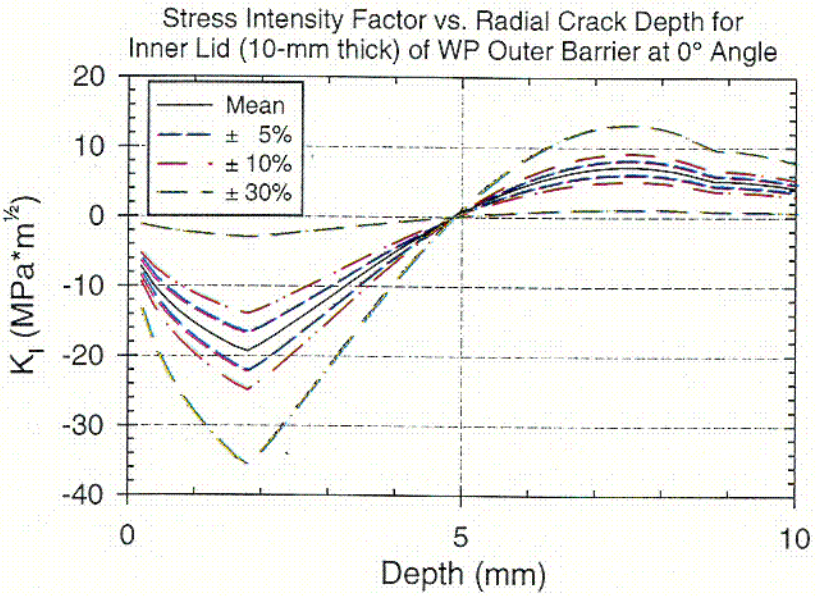

Figure 8. Stress intensity factor as a function of the projected radial crack depth in the flat closure lid welds (10-mm thick) at the reference location on the flat closure lid weld circumference and the uncertainty range.

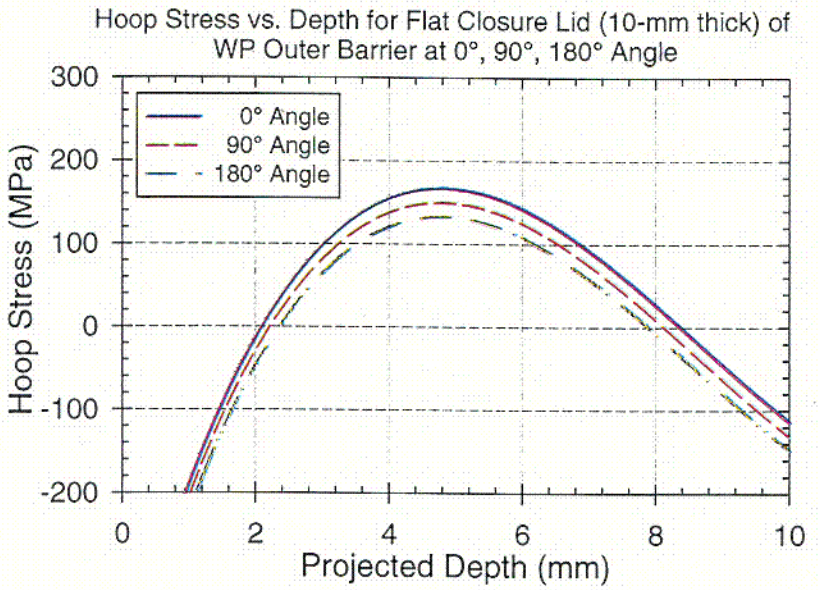

Figure 9. Hoop stress as a function of the projected depth in the flat closure lid welds (10-mm thick) at 0°, 90° and 180° angles along the circumference of the flat closure lid weld.

C05

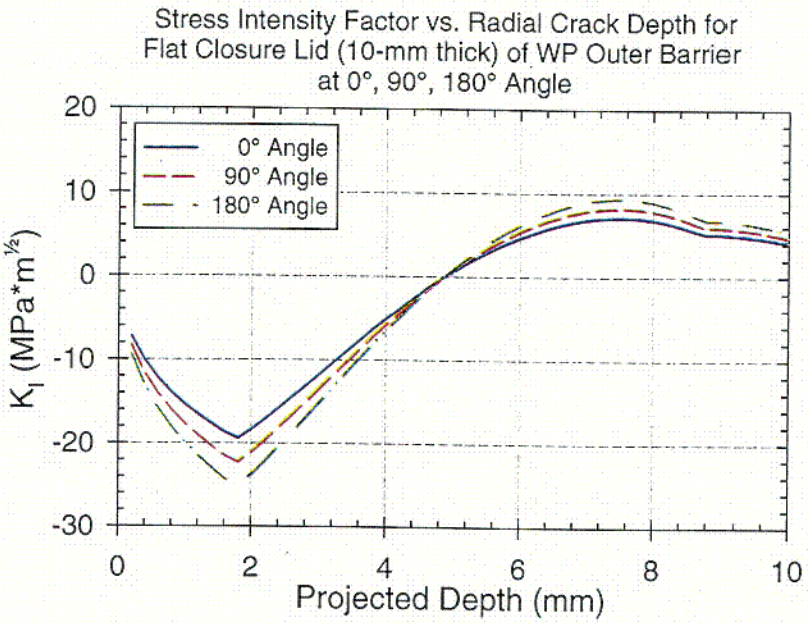

Figure 10. Stress intensity factor as a function of the projected radial crack depth in the flat closure lid welds (10-mm thick) at 0°, 90° and 180° angles along the flat closure lid weld circumference.

6.3.1.2 Abstraction Results and Discussion of Uncertainty Model 2 (Alternative Conservative Model)

The abstraction results for the uncertainty range (using Uncertainty Model 2) of the hoop stress at the weld centerline plane as a function of depth in the extended closure lid welds (25-mm thick) are given in Figure 11. The abstraction results discussed in this section result from analyses presented in Attachments II and III using 0.3 for the fraction of yield strength (F) and assuming (see Assumption 5.3.4) z is given by a triangular distribution. The stress profiles in Figure 11 are at a reference location ($0°$ angle) on the circumference of the lid welds. The figure shows that the hoop stress in the extended closure lid welds is compressive at the surface (from stress mitigation with the induction-heating solution annealing technique) and becomes tensile at a depth of 6 mm for the upper bound and 10 mm for the lower bound. The corresponding stress intensity factor profiles (using Uncertainty Model 2) as a function of radial crack depth are shown in Figure 12. The stress intensity factor is negative at the surface, consistent with the compressive stress at the surface shown in Figure 11, and becomes positive at a depth 3 mm for the +30% bounding case. No SCC crack growth will initiate until this layer is removed.

The abstraction results for the uncertainty range of the hoop stress as a function of the projected depth in the flat closure lid welds (10-mm thick) are given in Figure 13. The stress profiles are at a reference location ($0°$ angle) on the circumference of the lid welds. The hoop stress in the flat closure lid welds is compressive at the surface, transitions to tensile state at a projected depth between 1 and about 3 mm, and then back to compressive state at a projected depth between 6.8 and 9.8 mm. The corresponding stress intensity factor profiles as a function of the projected radial crack depth are shown in Figure 14. The stress intensity factor is negative at the surface and becomes positive at a projected depth of about 2 mm for the +30% bounding case. No SCC

C06

crack growth will initiate until this layer is removed. The uncertainty of the stress intensity factor increases slightly with the weld depth. Overall, the increased range of uncertainty of the input parameters to the stress corrosion cracking model should result in an increase in the range of SCC crack failure times as well as potentially earlier crack penetration times for both the extended and flat closure lids.

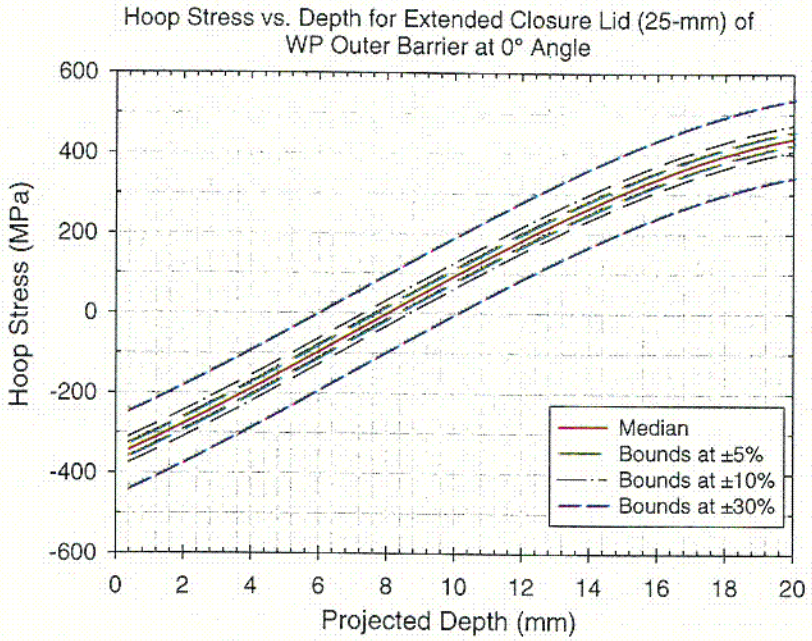

Figure 11. Hoop stress as a function of depth in the Alloy 22 extended closure lid welds (25-mm thick) at the reference location on the extended lid weld circumference using uncertainty bounds of ± 5, 10, and 30%

C07

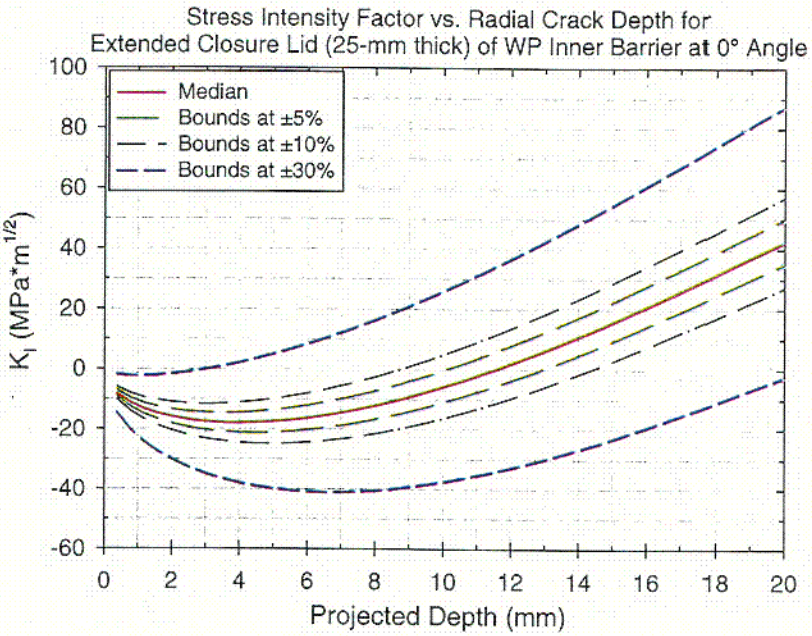

Figure 12. Stress intensity factor as a function of radial crack depth in the Alloy 22 extended closure lid welds (25-mm thick) at the reference location on the extended closure lid weld circumference using uncertainty bounds of ± 5, 10, and 30%

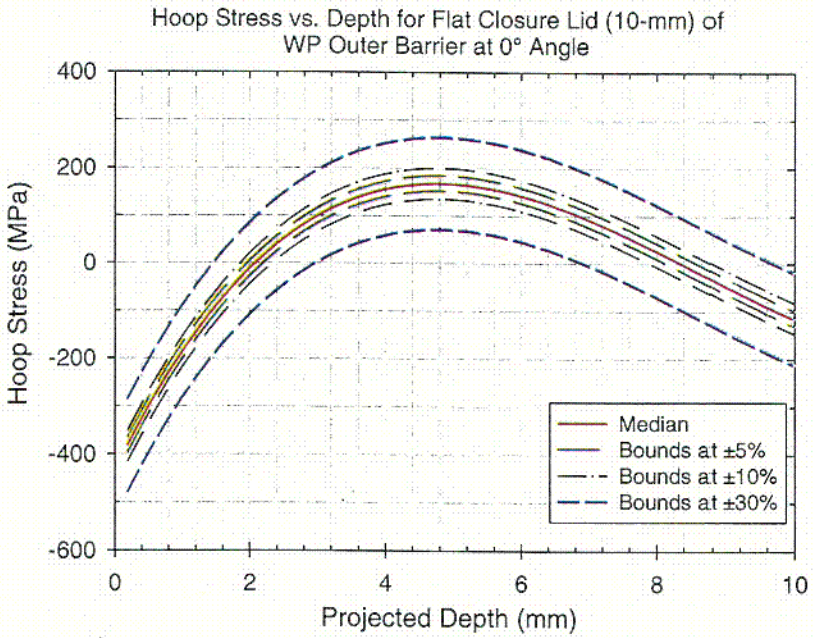

Figure 13. Hoop stress as a function of radial crack depth in the Alloy 22 flat closure lid welds (10-mm thick) at the reference location on the flat closure lid weld circumference using uncertainty bounds of ± 5, 10, and 30%

C08

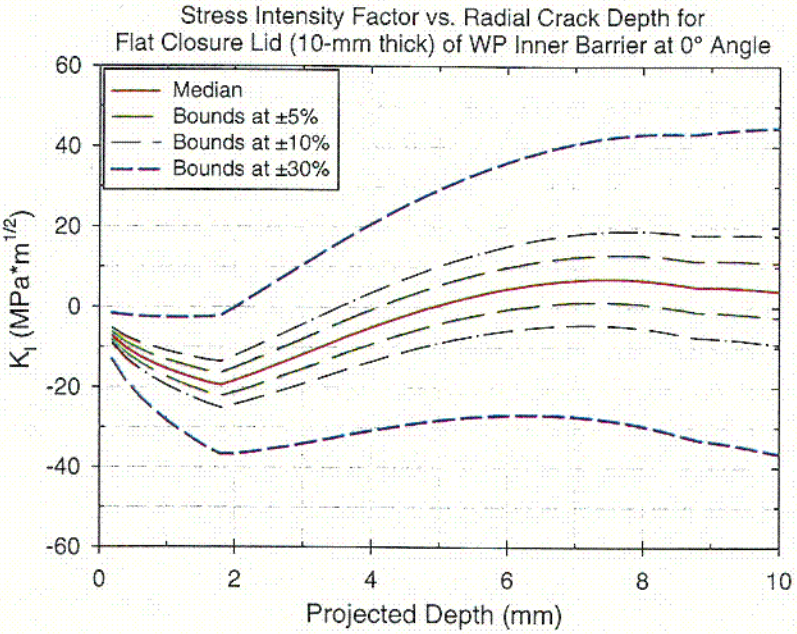

Figure 14. Stress intensity factor as a function of depth in the Alloy 22 flat closure lid welds (10-mm thick) at the reference location on the flat closure lid weld circumference using uncertainty bounds of ± 5, 10, and 30%

6.3.2 Stress and Stress Intensity Factor Profile Abstraction Model Validation

The Stress and Stress Intensity Factor Profile Abstraction Model (SSIFPAM) is an abstraction model. The validation method used in this section is to review the model parameters for reasonableness, or consistency in explanation of all relevant data. This results in an appropriate level of confidence in the SSIFPAM to consider it validated. As the SSIFPAM is an abstraction model, the only data relevant to this validation exercise is the process-level model being abstracted (CRWMS M&O 2000a, Section 6.2.2). Note that the SSIFPAM uses the same model parameters (with the exception noted in Section 4, Table 4, and Attachment I) and functional forms as its parent process-level model (CRWMS M&O 2000a, Section 6.2.2). The data used to develop the model parameters and functional forms are qualified (DTN: LL000316005924.140, LL000316105924.141). These observations are sufficient to validate the model inputs (i.e., the abstracted model is consistent with the process-level model). Therefore, the model inputs and functional forms are validated.

There are four figures in this AMR which are graphically similar to figures presented in upstream process level AMR (CRWMS M&O 2000a, Attachment I). Table 8 identifies these figures.

C09

Table 8. Figures to be compared between this AMR and the upstream process level AMR.

Figure in this AMR	Page Number of Figure in Process Level AMR
3	I-33
4	I-34
7	I-50
8	I-51

Note that the mean and ± 5% curves presented in the figures in this AMR are similar to those presented in Attachment I of the upstream process-level AMR (CRWMS M&O 2000a, Attachment I). This observation allows for two conclusions; the SSIFPAM model is implemented properly in Attachment II and Attachment III, and the SSIFPAM results agree with the process level model from which it was derived. The observations presented in this section result in an appropriate level of confidence in the model to consider it validated.

6.4 SLIP DISSOLUTION ABSTRACTION MODEL

The theory of slip dissolution (or film rupture) has been successfully applied to assess the SCC crack propagation for light water reactors at high temperature (CRWMS M&O 2000a, Section 6.4.1). The description of the SCC model based on the theory of slip dissolution and film rupture is discussed in the upstream process model analysis (CRWMS M&O 2000a, Section 6.4). The application of the slip dissolution model to assess the stress corrosion cracking behavior of the waste package outer barrier (Alloy 22) requires the determination of two parameters, A, the crack growth pre-exponent, and n, the repassivation slope, in an equation which relates the crack growth rate to the crack tip strain rate. A mathematical formula that relates A to n for stainless steels is adopted for Alloy 22 to determine A from n (CRWMS M&O 2000a, Section 6.4.4). Assumptions associated with this model are discussed in Section 5.4. This section discusses the approach and methodology used in the abstraction development for the slip dissolution model. This section also discusses the abstraction results and their implementation in the integrated waste package degradation model (WAPDEG) (CRWMS M&O 2000b, Section 6.3.13). The Slip Dissolution Abstraction Model documented in this technical product is potentially important to the evaluation of principle factors for the post-closure safety case, particularly those related to performance of the drip shield and waste package barriers. Therefore, this abstraction model has primary (Level 1) importance.

6.4.1 Abstraction Approach and Methodology

The purpose of this analysis is to develop abstractions for the parameters that are associated with the Slip Dissolution model. In the waste package degradation (WAPDEG) analysis this model is employed to calculate the growth rate of cracks initiated by stress corrosion cracking (SCC). The theory and fundamentals of the model are discussed in detail in the process model analysis (CRWMS M&O 2000a, Section 6.4). The waste package degradation analysis employs a stochastic approach to model the initiation and propagation of SCC cracks. The major efforts in the abstraction discussed in this section are to develop an approach to represent the uncertainty and variability associated with the SCC initiation and crack propagation processes, and to implement them in the waste package degradation analysis. As discussed in the following section, the associated parameters in the model include the two model parameters (A and n),

stress intensity factor (K_I), threshold stress, and incipient crack density and size. The nominal-case SCC analysis also includes pre-existing manufacturing defects in the closure lid welds. Abstractions for the manufacturing defects and the residual stress and stress intensity factor in the closure lid welds are discussed in Sections 6.2 and 6.3, respectively. The abstraction is based on a modeling approach that uses statistical sampling of the associated model parameter values within their probable range to capture the effects of the complex processes affecting the SCC crack initiation and growth rate.

6.4.2 Crack Growth Rate

The crack growth rate in the slip dissolution model is determined by the following expression (CRWMS M&O 2000a, Section 6.4.4).

$$V_t = \overline{A}(K_I)^{\overline{n}} \quad \text{(Eq. 28)}$$

where V is the crack growth rate in mm/s, and K_I is the stress intensity factor in MPa·m$^{1/2}$. Parameters, $\overline{A}$ and $\overline{n}$, in the above equation are expressed in terms of the repassivation slope, n, as follows (CRWMS M&O 2000a, Section 6.4.4).

$$\overline{A} = 7.8x10^{-2} n^{3.6} \left(4.1x10^{-14}\right)^n \quad \text{(Eq. 29)}$$

$$\overline{n} = 4n \quad \text{(Eq. 30)}$$

Parameter n (referred to as the repassivation slope) is a function of environmental and materials parameters such as solution conductivity, corrosion potential, and alloy composition (i.e., chromium depletion in the grain boundary) (CRWMS M&O 2000a, Section 6.4). The variability in the crack growth rate may be represented with potentially varying exposure conditions (incorporated through the repassivation slope, n) and stress intensity factor (K_I) among waste packages and also on different locations over a single waste package. However, due to a lack of data, n is considered independent of exposure conditions and alloy composition. In the waste package degradation analysis (CRWMS M&O 2000b, Section 6.1.13), the value of n is sampled from a range (i.e., from 0.75 to 0.84 or from 0.843 to 0.92 as discussed in the next paragraph). The impact of this approach needs to be assessed as additional data and analysis is developed. However, the effect of n on the failure time by SCC is less than the stress intensity factor (K_I) (see Section 6.4.5). As discussed in Section 6.3, the stress intensity factor profile (as a function of depth in the extended and flat closure lid welds) varies along the circumference of the closure lid welds, but the variability is not significant. It is assumed that there is no variability in the profile among waste packages (Assumption 5.3.5).

The uncertainty associated with the crack growth rate is represented with the uncertainties in the model parameters, i.e., n and K_I. As discussed in Section 6.3, the uncertainties associated with the K_I profiles in Uncertainty Models 1 and 2 are represented with triangular distributions with the mode at the mean profile and the bounds specified by the uncertainty range input. Because of a lack of data, the uncertainty associated with n is coarsely defined: uniform distribution between the lower bound 0.75 and the upper bound 0.84 (CRWMS M&O 2000a, Section 6.4.4). Incorporation of more recent data into the upstream AMR (CRWMS M&O 2000a, Section 6.4.4)

has resulted in revision of the uncertainty distribution bounds associated with n, i.e. a uniform distribution between 0.843 and 0.92.

6.4.3 Threshold Stress for Crack Growth Initiation

The threshold stress is defined as the minimum stress at which cracks start growing at a rate determined by Equation (2). The threshold stress may be represented as a fraction of the yield strength of the material, which varies with temperature (CRWMS M&O 1999c, Section 5.7). Because the upper limit of the temperature at which corrosion initiates (or stable liquid water can form) is 120.59°C (CRWMS M&O 2000f, Section 4.1.8, Table 7), the yield strength of Alloy 22 at 125°C is used. The yield strength was calculated by linearly interpolating the yield strengths at 93°C (338 MPa) and 204°C (283 MPa) (CRWMS M&O 1999c, Section 5.7) (DTN: MO0003RIB00071.000). The resulting yield strength used for the threshold stress is 322.3 MPa. Although the yield strength increases as temperature decreases, the value at 125 °C is used for all the waste package temperatures after corrosion initiates in the repository. This is because there is only a small change in the yield strength of Alloy 22 from 125 °C to the ambient temperature. Potentially marginal variability in the yield strength and thus the threshold stress are ignored in the current analysis.

As suggested in the process model analysis (CRWMS M&O 2000a, Section 6.5.2), the uncertainty in the threshold stress is conservatively represented as 20 to 30 percent of the yield strength, and uniform distribution is assumed for the uncertainty range. Thus, the resulting uncertainty range for the threshold stress is 64.46 to 96.60 MPa with the assumed uniform distribution between the two values. Incorporation of more recent data into the upstream AMR (CRWMS M&O 2000a, Section 6.5.2) has resulted in revision of the uncertainty distribution for the threshold stress to be a uniform distribution between 10 and 40 percent of the yield strength. The resulting uncertainty range for the threshold stress is 32.23 to 128.92 MPa. In the SCC analysis of waste package closure lid weld with WAPDEG, for each realization (or each run), the threshold stress is sampled from the range with the assumed uniform distribution, and the sampled threshold stress is used for all the closure lid weld patches of the waste packages under consideration.

6.4.4 Incipient Cracks and Manufacturing Defects

In the SCC process the crack initiation is associated with microscopic crack formation at localized corrosion or mechanical defect sites that are associated with pitting, intergranular attack, scratches, weld defects, planar dislocations, secondary phase precipitates, or design notches. The current analysis assumes that a crack depth range of about 20 μm to 50 μm represents the minimum crack depth for which the Slip Dissolution model can be applied. Those cracks are referred to as "incipient" cracks. Exponential distribution with a maximum size of 50 μm and a median size of 20 μm was suggested for the incipient crack size distribution (CRWMS M&O 2000a, Section 6.5.2). Because the effect of differing incipient crack sizes within the suggested range on crack growth rate is much less than the model parameters (n and K_I), the maximum crack size (50 μm) is used for all the incipient cracks considered in the SCC analysis.

The SCC analysis using the Slip Dissolution model also considers manufacturing defects in the closure lid welds. As discussed in Section 6.2, in the WAPDEG analysis, the size of the manufacturing defects are sampled for the closure lid weld patches, and the sampled defect flaws

are included in the Slip Dissolution model. Because manufacturing defects are much larger than the incipient cracks, the closure lid weld patches with manufacturing defects are likely to fail before closure lid weld patches without manufacturing defects.

6.4.5 Slip Dissolution Model Analysis

Bounding analyses were performed to examine the model responses for the SCC failure time of the extended closure lid (25-mm thick) and flat closure lid (10-mm thick) as a function of the model parameters (n and K_I). The analyses considered two bounding values (0.75 and 0.84) for n (CRWMS M&O 2000a, Sections 3.2 and 6.4.4) and a range of values for the stress intensity factor, which may be expected in the closure lid welds (CRWMS M&O 2000a, Attachment I). The threshold stress for crack growth initiation and pre-existing manufacturing defect were not considered in this bounding analysis. The results are shown in Figure 15. As shown in the figure, the stress intensity factor is the dominant parameter in the model, and the time to failure by SCC increases exponentially as the stress intensity factor decreases. The failure time by SCC is less than 100 years for the stress intensity factors greater than 20 MPa·m^{½}. The failure time increases to above 1,000 years if the stress intensity factor is kept below 6 MPa·m^{½}. The analysis demonstrates that, once a SCC crack initiates, it penetrates the closure lid thickness fast. It also demonstrates importance of stress mitigation in the closure lid welds to avoid potential early failures of waste packages by SCC.

A similar bounding analysis is considered for the latest distribution for n (uniform between 0.843 and 0.92) (CRWMS M&O 2000a, Sections 3.2 and 6.4.4). In Figure 15, the curves for n = 0.84 are suitable for evaluation of the lower bound (0.843). As shown in the figure, the failure time by SCC is less than 100 years for the stress intensity factors greater than 30 MPa·m^{½}. The failure time increases to above 6,000 years if the stress intensity factor is kept below 6 MPa·m^{½}.

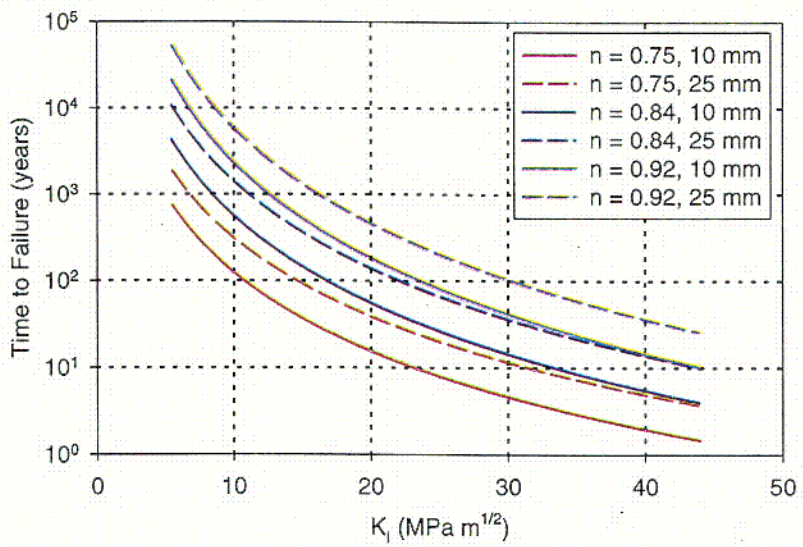

Figure 15. Bounding calculations for the model responses for the time to failure of the extended and flat closure lids by SCC calculated with the slip dissolution model using the bounding values for parameter n for a range of the stress intensity factor values.

C10

6.4.6 Slip Dissolution Abstraction Model Validation

The Slip Dissolution Abstraction Model (SDAM) is an abstraction model. The validation method used in this section is to review the model parameters for reasonableness, or consistency in explanation of all relevant data. This results in an appropriate level of confidence in the SDAM to consider it validated. As the SDAM is an abstraction model, the only data relevant to this validation exercise is the process-level model being abstracted (CRWMS M&O 2000a, Section 6.4.4). Note that the SDAM uses the same model parameters and functional forms as its parent process-level model (CRWMS M&O 2000a, Section 6.4.4). The fact that the functional forms and model parameters used in the SDAM are identical to those provided in the process-level model is considered sufficient to validate the model inputs (i.e., the abstracted model is consistent with the process-level model). Therefore, the model inputs are validated and the model is implemented within qualified software. This results in an appropriate level of confidence in the model to consider it validated.

6.5 THRESHOLD STRESS INTENSITY FACTOR ABSTRACTION MODEL

The concept of threshold stress intensity factor (K_{ISCC}) has been commonly used to assess the susceptibility of material to SCC (CRWMS M&O 2000a, Section 3.2). A description of this concept is discussed in the upstream process model analysis (CRWMS M&O 2000a, Section 6.3). According to the threshold model, there exists a threshold value (K_{ISCC}) for the stress intensity factor such that no growth occurs in a pre-existing crack having an initial stress intensity factor at the crack tip less than the threshold value. Pre-existing cracks are usually caused by manufacturing processes (especially welding processes). The Threshold Stress Intensity Factor Abstraction Model documented in this technical product is potentially important to the evaluation of principle factors for the post-closure safety case, particularly those related to performance of the drip shield and waste package barriers. Therefore, this abstraction model has primary (Level 1) importance.

The applicability of this model to the waste package outer barrier (Alloy 22) has been studied experimentally and estimates of K_{ISCC} have been obtained. A reasonable mean value of 30 ksi·in$^{1/2}$ was estimated using load controlled compact tension specimens exposed to 110°C basic saturated water (BSW) (CRWMS M&O 2000a, Section 6.3.2). This mean value was corroborated (Roy et al. 1998) along with an experimental basis for establishing the expected degree of uncertainty. In this latter study the susceptibility of Alloy 22 and Ti Grade 12 to SCC is evaluated by using wedge-loaded pre-cracked double-cantilever-beam (DCB) specimens in de-aerated acidic brine (pH ≈ 2.7) at 90°C. Details of the testing and model are described by Roy et al. (1998).

In this model failure is assumed to occur for crack sizes a where $K_I \geq K_{ISCC}$. In applying the Threshold Stress Intensity Factor model, it is necessary to obtain information on (1) stress intensity factor $K_I(a, \sigma)$ as a function of crack size correspondent to the stress state at and near the crack site and (2) the threshold value of the stress intensity factor K_{ISCC}. This method is potentially conservative because it ignores the fact that the crack growth does not necessarily lead to a failure state in cases where the stress intensity factor exceeds the threshold value.

As suggested in the process model analysis (CRWMS M&O 2000a, Section 6.3), the K_{ISCC} of the waste package outer barrier (Alloy 22) is characterized assuming a normal distribution with a

mean of 30 ksi·in$^{1/2}$ (or 33 MPa·m$^{1/2}$) and a standard deviation of 1.6 ksi·in$^{1/2}$ (or 1.8 MPa·m$^{1/2}$). It is assumed the distribution is bounded at ± 4 standard deviations. The entire variance of the K_{ISCC} is considered as uncertainty. The probability density function for the K_{ISCC} is shown in Figure 16. The lower limit of the parameter is 23.5 ksi·in$^{1/2}$ (or 25.9 MPa·m$^{1/2}$), and the upper limit is 36.5 ksi·in$^{1/2}$ (or 40.2 MPa·m$^{1/2}$). Additional data are needed for the effect of different exposure conditions (including applied stress) on the K_{ISCC} value, and to better quantify its uncertainty and variability under those varying exposure conditions (CRWMS M&O 2000a, Section 6.3.2).

As shown in Figure 2, the maximum possible manufacturing defect flaw size that could realistically be sampled in the closure lid welds is about 6-mm. Assuming this defect flaw is a radial crack, the maximum stress intensity factor at the tip of the crack in the extended closure lid is about 10 MPa·m$^{1/2}$ (Figure 12), and that in the flat closure lid is about 37 MPa·m$^{1/2}$ (Figure 14). Since the maximum stress intensity factor at the tip of the crack in the extended closure lid weld region is below the lower limit of the threshold stress intensity factor distribution, the Threshold Stress Intensity Factor Abstraction Model predicts no SCC in the 25-mm thick extended closure lid weld region. The model does predict the possibility of immediate failure of the thinner 10-mm flat closure lid. However, waste package breach would be significantly delayed by the time required for general corrosion to penetrate the 25-mm thick extended closure lid and allow for SCC initiation in the flat closure lid.

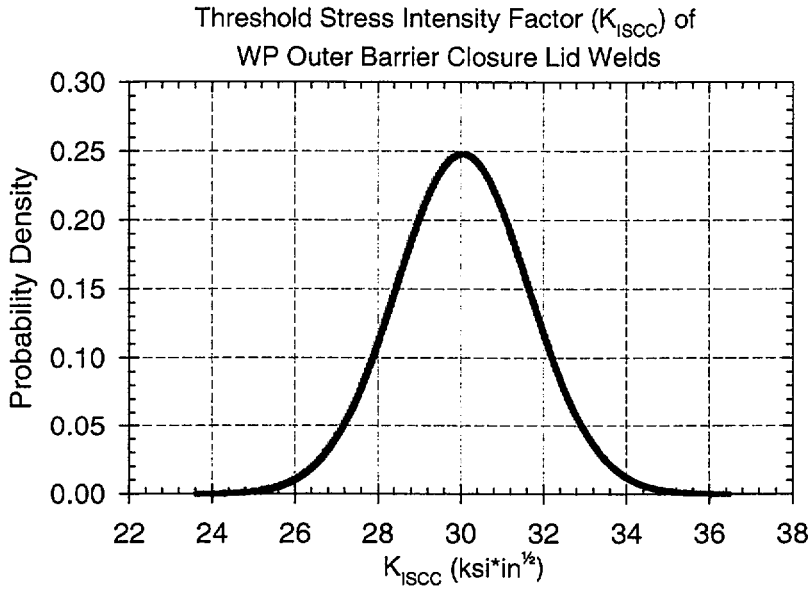

Figure 16. Probability density function of the threshold stress intensity factor of the waste package outer barrier closure lids (Alloy 22).

6.5.1 Threshold Stress Intensity Factor Abstraction Model Validation

The Threshold Stress Intensity Factor Abstraction Model (TSIFAM) is an abstraction model. The validation method used in this section is to review the model parameters for reasonableness, or consistency in explanation of all relevant data. This results in an appropriate level of confidence in the TSIFAM to consider it validated. As the TSIFAM is an abstraction model, the only data

relevant to this validation exercise is the process-level model being abstracted (CRWMS M&O 2000a, Section 6.3). Note that the SDAM uses the same model parameters and functional forms as its parent process-level model (CRWMS M&O 2000a, Section 6.3). The fact that the functional forms and model parameters used in the SDAM are identical to those provided in the process-level model is considered sufficient to validate the model inputs (i.e., the abstracted model is consistent with the process-level model). Therefore, the model inputs and are validated and the model is implemented within qualified software. This results in an appropriate level of confidence in the model to consider it validated.

7. CONCLUSIONS

The results of the abstraction analyses documented in this AMR are tracked by DTN: MO0010MWDSUP04.010 (Stress Corrosion Cracking analyses results) and DTN: MO0010SPASUP04.011 (Manufacturing Defect Model analyses results).

Hydrogen induced cracking (HIC) of drip shield is a potential degradation mechanism that could cause failure of the drip shield if the hydrogen uptake in the titanium drip shield is greater than the critical hydrogen concentration and in the presence of applied stress (CRWMS M&O 2000d, Section 7). Crevice corrosion, passive general corrosion, and galvanic couple formation are three feasible processes in the repository that could lead to HIC of the drip shield. Hydrogen is produced as a result of the corrosion processes and some of the produced hydrogen can be absorbed by and transport into the titanium drip shield (CRWMS M&O 2000d, Section 6.1.5). Because the drip shield will not be subject to crevice corrosion under the exposure conditions anticipated in the repository (CRWMS M&O 2000d, Section 6.1.4), general corrosion and galvanic couple formation are the only mechanisms that could cause HIC in the drip shield. Results of the bounding analyses have shown that the time that the hydrogen uptake concentration reaches the critical hydrogen concentration from passive corrosion under the repository exposure conditions is greater than 10,000 years (CRWMS M&O 2000d, Section 6.2.3). Galvanic couples should be local in effect, short lived in duration, and unlikely to produce hydrogen in sufficient quantities to exceed the critical hydrogen concentration. Furthermore, any crack openings in the drip shield are expected to quickly become plugged with corrosion products and/or other mineral precipitates leading to very little water transport. Therefore no additional abstraction analysis was conducted for HIC of drip shield.

In order for stress corrosion cracking (SCC) to occur, the following three factors must be present: metallurgical susceptibility, critical environment, and a static (or sustained) tensile stress (CRWMS M&O 2000a, Section 6.1). Both the drip shield material (Ti Grade 7) and the waste package outer barrier material (Alloy 22) are susceptible to SCC. A critical environment is assumed always present. Therefore, all that is required for SCC is the presence of a tensile stress state. The drip shield is assumed to be fully stress-relief annealed before it is placed in the emplacement drift and is therefore not subject to SCC unless subjected to mechanical loading due to rockfall. Any crack openings in the drip shield formed due to rockfall-induced stress states are expected to quickly become plugged with corrosion products and/or other mineral precipitates leading to very little water transport (CRWMS M&O 2000a, Section 6.5.5). Therefore no additional abstraction analysis was conducted for SCC of drip shield. For SCC of waste package, except the welds for the closure (extended and flat) lids, all the fabrication welds in the waste packages are assumed fully annealed and not subject to SCC. Accordingly, analyses

were conduced to develop abstractions for the SCC models and parameters for the waste package closure lid welds. The abstractions developed in the current analyses are: 1) stress and stress intensity factor profiles as a function of depth, 2) threshold stress intensity factor, 3) threshold stress to initiate crack growth, 4) parameters A and n of the Slip Dissolution model, 5) incipient crack density and size used with the Slip Dissolution Model, and 6) probability for the occurrence and size of manufacturing defects in the closure lid welds. Major efforts of the abstraction were given to develop an approach to represent uncertainty and variability of the model parameters.

In the current waste package degradation analysis, two alternative SCC models, the Slip Dissolution (or Film Rupture) Model and the Threshold Stress Intensity Factor (K_{ISCC}) Model, are considered (CRWMS M&O 2000a, Section 3.2). In the Threshold Stress Intensity Factor Model, the threshold stress intensity factor (K_{ISCC}) is used to determine if SCC will occur. Provided that an initial flaw and corrosive environment is present, a SCC failure will occur if the applied stress intensity factor K_I is greater than or equal to the threshold stress intensity factor K_{ISCC} (i.e., $K_I \geq K_{ISCC}$). The Slip Dissolution Model assumes that incipient cracks and manufacturing defects grow continuously when the oxidation reaction that occurs at the crack tip ruptures the protective film via an applied strain in the underlying matrix. The rate at which the crack grows is a function of the crack tip strain rate, environmental conditions, and material properties.

The possible maximum manufacturing defect size in the closure lid welds is about 6-mm (Figure 2). Assuming this defect flaw is a radial crack, the maximum stress intensity factor at the tip of the manufacturing defect in the extended closure lid is about 10 MPa·m^{½} (Figure 12), and that in the flat closure lid is about 37 MPa·m^{½} (Figure 14). Because the maximum stress intensity factor at the tip of a manufacturing defect in the extended closure lid is below the minimum K_{ISCC} value, the Threshold Stress Intensity Factor Model predicts SCC will not occur in the extended closure lid weld region and waste package breach would be significantly delayed by the time required for general corrosion to penetrate the 25-mm thick extended closure lid. For this reason, the Slip Dissolution Model is the more conservative of the two models considered and should be used to model waste package performance in the potential repository.

The Slip Dissolution Model has been successfully applied to assess the SCC crack propagation for light water reactors at high temperature (CRWMS M&O 2000a, Section 6.4.1). The Slip Dissolution Model assumes that SCC cracks grow continuously in the presence of stress. Analyses were conducted to develop abstractions for the parameters that are associated with the Slip Dissolution Model. The major efforts in the abstractions were to develop an approach to represent the uncertainty and variability associated with the SCC initiation and crack propagation processes, and to implement them in the integrated waste package degradation model (WAPDEG model) (CRWMS M&O 2000b, Section 6.3.12 and 6.3.13). Utilizing the data and models from the process model analyses, abstractions were developed for the parameters associated with the model. Those parameters include two model parameters (A and n), stress intensity factor (K_I), threshold stress, incipient crack density and size, and probability of occurrence and size of pre-existing manufacturing defects in the closure lid welds.

Bounding analyses were performed to examine the responses of the Slip Dissolution model for the SCC failure time of the extended closure lid (25-mm thick) and flat closure lid (10-mm thick) as a function of the model parameters (n and K_I). It was shown in the analyses that the stress

intensity factor is the dominant parameter in the model, and the time to failure by SCC increases exponentially as the stress intensity factor decreases. Once a SCC crack initiates, it penetrates the closure lid thickness fast. The analysis also demonstrated importance of stress mitigation in the closure lid welds to avoid potential early failures of waste packages by SCC.

This document may be affected by technical product input information that requires confirmation. Any changes to the document that may occur as a result of completing the confirmation activities will be reflected in subsequent revisions. The status of the input information quality may be confirmed by review of the Document Input Reference System database.

8. INPUTS AND REFERENCES

8.1 DOCUMENT CITED

Budnitz, B.; Ewing, R.C.; Moeller, D.W.; Payer, J.; Whipple, C.; and Witherspoon, P.A. 1999. *Peer Review of the Total System Performance Assessment-Viability Assessment Final Report.* Las Vegas, Nevada: Total System Performance Assessment Peer Review Panel. ACC: MOL.19990317.0328.

CRWMS M&O (Civilian Radioactive Waste Management System Management and Operating Contractor) 1999a. *Model Abstractions to Support WAPDEG Analysis of Waste Package and Drip Shield Degradation.* TDP-EBS-PA-000002 REV 00. Las Vegas, Nevada: CRWMS M&O. ACC: MOL.19991008.0223.

CRWMS M&O 1999b. *Conduct of Performance Assessment.* Activity Evaluation, September 30, 1999. Las Vegas, Nevada: CRWMS M&O. ACC: MOL.19991028.0092.

CRWMS M&O 1999c. *Waste Package Materials Properties.* BBA000000-01717-0210-00017 REV 00. Las Vegas, Nevada: CRWMS M&O. ACC: MOL.19990407.0172.

CRWMS M&O 2000a. *Stress Corrosion Cracking of the Drip Shield, the Waste Package Outer Barrier and the Stainless Steel Structural Material.* ANL-EBS-MD-000005 REV 00 ICN 01. Las Vegas, Nevada: CRWMS M&O. ACC: MOL.20001102.0340.

CRWMS M&O 2000b. *WAPDEG Analysis of Waste Package and Drip Shield Degradation.* ANL-EBS-PA-000001 REV 00. Las Vegas, Nevada: CRWMS M&O. ACC: MOL.20000526.0332.

CRWMS M&O 2000c. *Calculation of Probability and Size of Defect Flaws in Waste Package Closure Welds to Support WAPDEG Analysis.* CAL-EBS-PA-000003 REV 00. Las Vegas, Nevada: CRWMS M&O. ACC: MOL.20000424.0676.

CRWMS M&O 2000d. *Hydrogen Induced Cracking of Drip Shield.* ANL-EBS-MD-000006 REV 00 ICN 01. Las Vegas, Nevada: CRWMS M&O. ACC: MOL.20001025.0100.

CRWMS M&O 2000e. *General Corrosion and Localized Corrosion of the Drip Shield.* ANL-EBS-MD-000004 REV 00. Las Vegas, Nevada: CRWMS M&O. ACC: MOL.20000329.1185.

CRWMS M&O 2000f. *Environment on the Surfaces of the Drip Shield and Waste Package Outer Barrier.* ANL-EBS-MD-000001 REV 00. Las Vegas, Nevada: CRWMS M&O. ACC: MOL.20000328.0590.

CRWMS M&O 2000g. *Analysis of Mechanisms for Early Waste Package Failure.* ANL-EBS-MD-000023 REV 01. Las Vegas, Nevada: CRWMS M&O. ACC: MOL.20000223.0878.

CRWMS M&O 2000h. *Monitored Geologic Repository Project Description Document.* TDR-MGR-SE-000004 REV 02. Las Vegas, Nevada: CRWMS M&O. ACC: MOL.20001031.0062.

CRWMS M&O 2000i. *Analysis of Mechanisms for Early Waste Package Failure.* ANL-EBS-MD-000023 REV 02. Las Vegas, Nevada: CRWMS M&O. ACC: MOL.20001011.0196.

CRWMS M&O 2000j. Process Control Evaluation For Supplement V: "Performance Assessment Operations. (Reference QAP-2-0 Activity Evaluation Form. Conduct of Performance Assessment, November 9, 1999)". Las Vegas, Nevada: CRWMS M&O. ACC: MOL.20000128.0236.

Roy, A. K., Fleming, D.L., Freeman, D.C., and Lum, B.Y. 1998. *Stress Corrosion Cracking of Alloy C-22 and Ti GR-12 Using Double-Cantilever-Beam Technique.* UCRL-JC-132145. Livermore, California: Lawrence Livermore National Laboratory. ACC: MOL.19990420.0114.

8.2 CODES, STANDARDS, REGULATIONS, AND PROCEDURES

AP-SI.1Q, Rev. 2, ICN 4, ECN 1. *Software Management.* Washington, D.C.: Department of Energy, Office of Civilian Radioactive Waste Management. ACC: MOL.20001019.0023.

AP-SV.1Q, Rev. 0, ICN 2. *Control of the Electronic Management of Information.* Washington, D.C.: U.S. Department of Energy, Office of Civilian Radioactive Waste Management. ACC: MOL.20000831.0065.

DOE (U.S. Department of Energy) 2000. *Quality Assurance Requirements and Description.* DOE/RW-0333P, Rev. 10. Washington, D.C.: U.S. Department of Energy, Office of Civilian Radioactive Waste Management. ACC: MOL.20000427.0422.

Kotra, J.P.; Lee, M.P.; Eisenberg, N.A.; and DeWispelare, A.R. 1996. *Branch Technical Position on the Use of Expert Elicitation in the High-Level Radioactive Waste Program.* NUREG-1563. Washington, D.C.: U.S. Nuclear Regulatory Commission. TIC: 226832

NLP-2-0, Rev. 5. *Determination of Importance Evaluations.* Las Vegas, Nevada: CRWMS. ACC: MOL.19981116.0120.

NRC (U.S. Nuclear Regulatory Commission) 1999. *Issue Resolution Status Report Key Technical Issue: Container Life and Source Term.* Rev. 2. Washington, D.C.: U.S. Nuclear Regulatory Commission. TIC: 245538

QAP-2-0, Rev. 5. *Conduct of Activities.* Las Vegas, Nevada: CRWMS M&O. ACC: MOL.19980826.0209.

QAP-2-3, Rev. 10. *Classification of Permanent Items*, Las Vegas, Nevada: CRWMS M&O. MOL 19990316.006.

YAP-SV.1Q, Rev. 0, ICN 1. *Control of the Electronic Management of Data.* Washington, D.C.: U.S. Department of Energy, Office of Civilian Radioactive Waste Management. ACC: MOL.19991008.0209.

8.3 SOURCE DATA, LISTED BY DATA TRACKING NUMBER

MO0001SPASUP03.001. Data to Support Calculation of Probability and Size of Defect Flaws in Waste Package Closure Welds to Support WAPDEG Analysis. CAL-EBS-PA-000003 REV 00. Submittal date: 01/31/2000.

MO0003RIB00071.000. Physical and Chemical Characteristics of Alloy 22. Submittal date: 03/13/00.

LL000316005924.140. Stress Corrosion Cracking of the Drip Shield, The Waste Package Outer Barrier and the Stainless Steel Structural Material. Submittal date: 03/22/2000

LL000316105924.141. Stress Corrosion Cracking of the Drip Shield, The Waste Package Outer Barrier and the Stainless Steel Structural Material. Submittal date: 03/22/2000.

9. ATTACHMENTS

I - Hoop Stress Coefficient Comparison for Extended Closure Lid (25 mm lid)

II - Uncertainty and Variability Models – Extended Closure Lid

III - Uncertainty and Variability Models – Flat Closure Lid

Attachment I

Hoop Stress Coefficient Comparison for Extended Closure Lid (25mm lid)

The purpose of this worksheet is to compare the stress coefficients used in the WAPDEG model as document in Section 4 to the stress coefficients that were submitted in DTN: LL000316005924.140

Conversion Factors: 1 in = 25.4 mm, 1 ksi = 6.894757 MPa, 1 ksi-in^½ = 1.098843 MPa-m^½ (from DTN: LL000316005924.140, File: S&K_OL_Anne.xls, Worksheet: Anneal,Sz, Cells: A82 to M82

$c0 := 25.4$

$c1 := 6.894757$

$c2 := 1.098843$

Coefficients used in the WAPDEG Model:

Non-Metric	Convert to Metric	Value in Metric Units
$C_0 := -51.672275$	$A_0 := C_0 \cdot c1$	$A_0 = -356.26778$
$C_1 := 136.97241$	$A_1 := C_1 \cdot \frac{c1}{c0}$	$A_1 = 37.180767$
$C_2 := 134.40677$	$A_2 := C_2 \cdot \frac{c1}{c0 \cdot c0}$	$A_2 = 1.436391$
$C_3 := -155.15755$	$A_3 := C_3 \cdot \frac{c1}{c0 \cdot c0 \cdot c0}$	$A_3 = -0.065282$

Coefficients from DTN: LL000316005924.140 File: S&K_OL_Anne.xls, Worksheet: Anneal,Sz, Cells: C9 to C13

Non-Metric	Convert to Metric	Value in Metric Units
$D_0 := -51.6776$	$E_0 := D_0 \cdot c1$	$E_0 = -356.304494$
$D_1 := 137$	$E_1 := D_1 \cdot \frac{c1}{c0}$	$E_1 = 37.188256$
$D_2 := 134.367$	$E_2 := D_2 \cdot \frac{c1}{c0 \cdot c0}$	$E_2 = 1.435966$
$D_3 := -155.147$	$E_3 := D_3 \cdot \frac{c1}{c0 \cdot c0 \cdot c0}$	$E_3 = -0.065277$

The two stress functions below evaluate the stress profiles obtained using the different sets of coefficients:

$\sigma 1_s(x) := A_0 + A_1 \cdot x + A_2 \cdot x^2 + A_3 \cdot x^3$ $\sigma 2_s(x) := E_0 + E_1 \cdot x + E_2 \cdot x^2 + E_3 \cdot x^3$

$xx := 0..20$ Evaluate between 0 and 20 mm

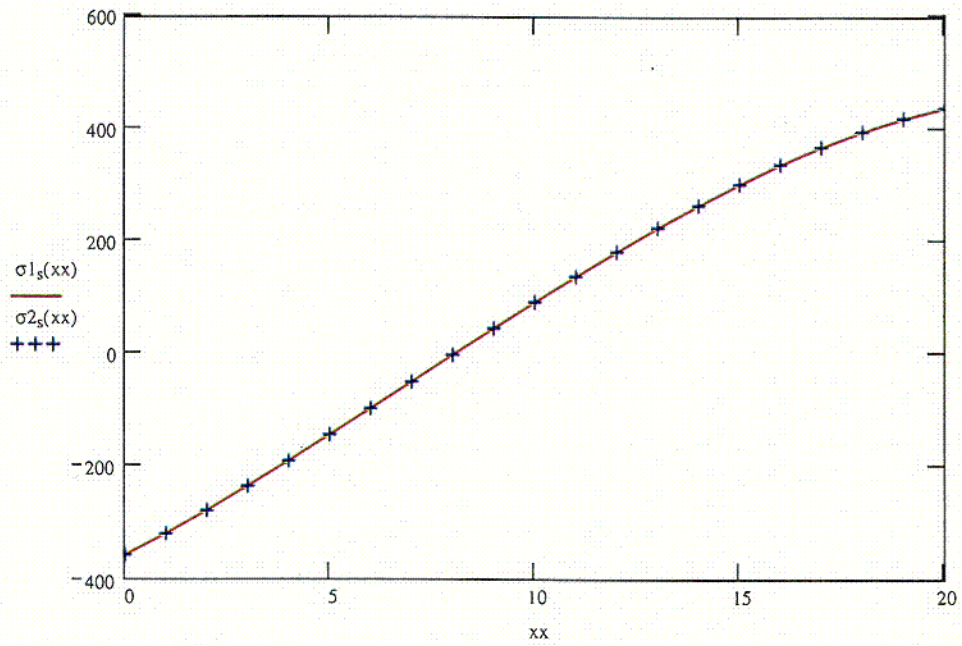

The two stress profiles are quite similar.

C11

The relative error between the profiles is:

$$RE_{xx} := \frac{\sigma 1_s(xx) - \sigma 2_s(xx)}{\sigma 2_s(xx)}$$

It is concluded that these minor variations in stress profile will have no significant effect on the analysis.

$$RE = \begin{pmatrix} -1.03042711 \times 10^{-4} \\ -9.33008624 \times 10^{-5} \\ -8.45686783 \times 10^{-5} \\ -7.68572989 \times 10^{-5} \\ -7.03237668 \times 10^{-5} \\ -6.54802714 \times 10^{-5} \\ -6.40413327 \times 10^{-5} \\ -7.48388566 \times 10^{-5} \\ -5.42887114 \times 10^{-3} \\ 1.06559745 \times 10^{-5} \\ -1.22206347 \times 10^{-6} \\ -1.05890695 \times 10^{-6} \\ 2.04475135 \times 10^{-6} \\ 6.31826243 \times 10^{-6} \\ 1.12079259 \times 10^{-5} \\ 1.65102203 \times 10^{-5} \\ 2.21573285 \times 10^{-5} \\ 2.81477258 \times 10^{-5} \\ 3.45208987 \times 10^{-5} \\ 4.13490616 \times 10^{-5} \\ 4.8737355 \times 10^{-5} \end{pmatrix}$$

Attachment II

Uncertainty and Variability Models - Extended Closure Lid

Input values:

$$a := \begin{pmatrix} -356.26778 \\ 37.180767 \\ 1.436391 \\ -0.065282 \end{pmatrix}$$ Stress Coefficients

$YS := 322.3$ Yield Strength in MPa

Ktable :=

-8.0969	0.3988
-11.089	0.8001
-13.127	1.1989
-14.624	1.6002
-15.741	1.999
-16.565	2.4003
-17.166	2.7991
-17.57	3.2004
-17.795	3.5992
-17.86	3.998
-17.778	4.3993
-17.561	4.7981
-17.228	5.1994
-16.785	5.5982
-16.234	5.9995
-15.582	6.3983
-14.833	6.797
-13.992	7.1984
-13.062	7.5971
-12.038	7.9985
-10.931	8.3972
-9.7473	8.7986
-8.4893	9.1973
-7.1611	9.5987
-5.7664	9.9974
-4.3273	10.3962
-2.8308	10.7975
-1.2804	11.1963
0.32026	11.5976
1.96775	11.9964
3.65854	12.3977
5.4151	12.7965
7.21878	13.1978
9.05769	13.5966
10.9283	13.9954
12.8269	14.3967
14.7499	14.7955
16.7318	15.1968
18.7699	15.5956
20.8229	15.9969
22.8865	16.3957
24.9569	16.7945
27.0302	17.1958
29.1346	17.5946
31.3333	17.9959
33.5256	18.3947
35.707	18.796
37.8729	19.1948
40.0187	19.5961
42.1395	19.9949

$K := Ktable^{\langle 0 \rangle}$

$x := Ktable^{\langle 1 \rangle}$

This is the stress intensity factor (MPa m½) (column 0) versus depth (mm) (column 1).

$F := 0.3$ The maximum fraction of yield stress

$$sz(z) := \frac{z \cdot YS \cdot F}{3}$$

The uncertainty scaling factor.
z = ± 0.5 yields the ± 5% bounds
z = ± 1.0 yields the ± 10% bounds
z = ± 3.0 yields the ± 30% bounds

$s(x,\theta) := \left[a_0 + x\cdot\left[a_1 + x\cdot\left(a_2 + x\cdot a_3\right)\right]\right] - (2.5\cdot 6.894757)\cdot(1 - \cos(\theta))$ Stress as a function of depth, x, and angle, θ.

$depth := x$

$xf := x_{last(x)}$ The last entry in the stress intensity factor table is considered the total thickness for this calculation since this is the largest thickness for which data is available.

Uncertainty Model 1 - Variation with z

$$s_{u1}(\theta, z) := \overrightarrow{s(x,\theta)}\cdot\left(\frac{s(xf,\theta) + sz(z)}{s(xf,\theta)}\right)$$ Stress

$$K_{u1}(\theta, z) := K\cdot\frac{s(xf,\theta) + sz(z)}{s(xf,0)}$$ Stress Intensity Factor

Stresses evaluated at various values of z, i.e., z = ± 0.5, ± 1, and ± 3 at θ = 0°.

$out1^{\langle 0\rangle} := depth$

$out1^{\langle 1\rangle} := s_{u1}(0,0)$

$out1^{\langle 2\rangle} := s_{u1}(0,0.5)$

$out1^{\langle 3\rangle} := s_{u1}(0,-0.5)$

$out1^{\langle 4\rangle} := s_{u1}(0,1)$

$out1^{\langle 5\rangle} := s_{u1}(0,-1)$

$out1^{\langle 6\rangle} := s_{u1}(0,3)$

$out1^{\langle 7\rangle} := s_{u1}(0,-3)$

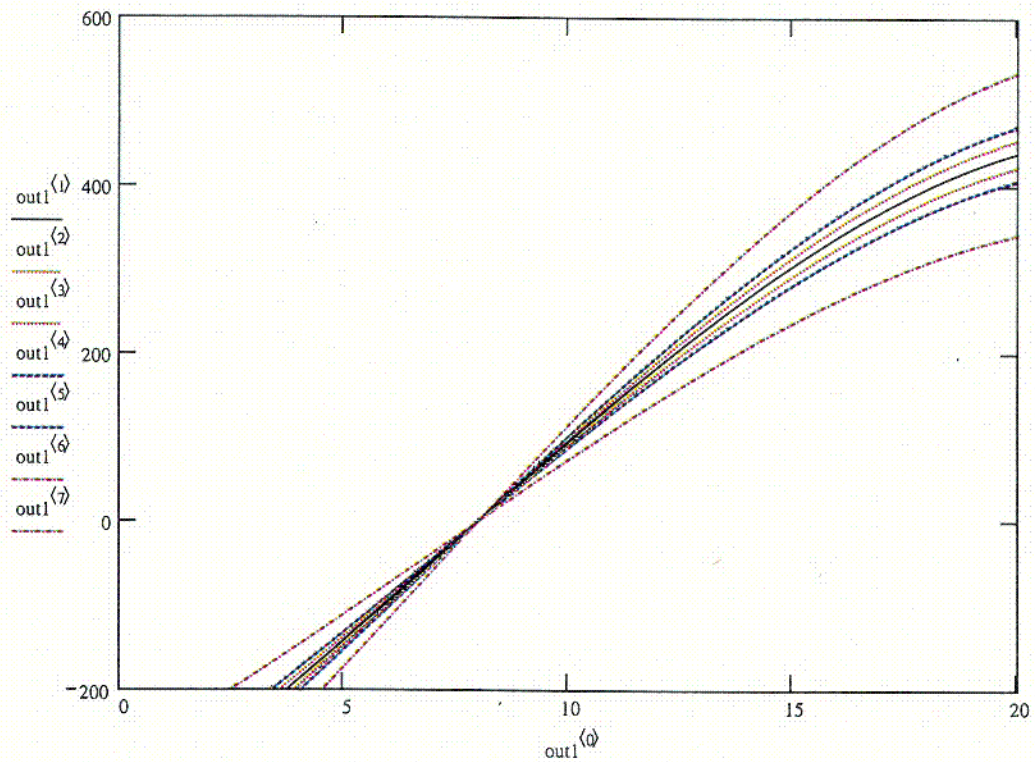

$out1^{\langle 8 \rangle} := K_{u1}(0,0)$ $out1^{\langle 12 \rangle} := K_{u1}(0,-1)$

$out1^{\langle 9 \rangle} := K_{u1}(0,0.5)$ $out1^{\langle 13 \rangle} := K_{u1}(0,3)$

$out1^{\langle 10 \rangle} := K_{u1}(0,-0.5)$ $out1^{\langle 14 \rangle} := K_{u1}(0,-3)$

$out1^{\langle 11 \rangle} := K_{u1}(0,1)$

Stress Intensity Factors evaluated at various values of z, i.e.,
z = ± 0.5, ± 1, and ± 3 at θ = 0°.

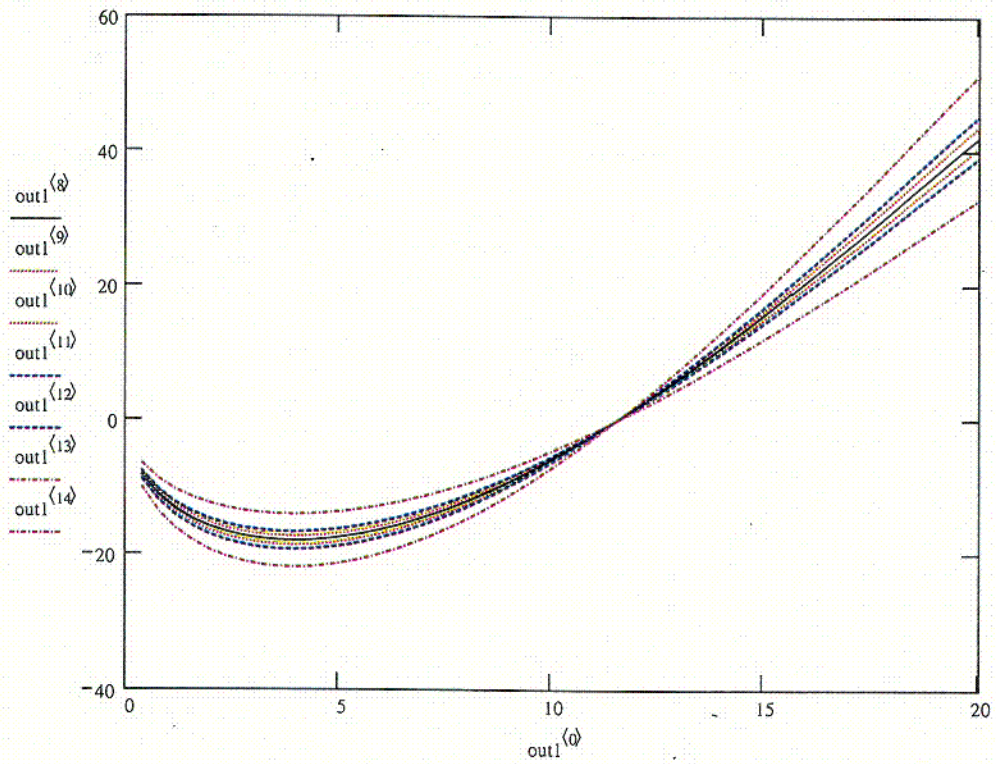

C13

Uncertainty Model 1 - Variation with angle, θ

$out1^{\langle 15 \rangle} := s_{u1}(90 \cdot deg, 0)$ $out1^{\langle 16 \rangle} := s_{u1}(180 \cdot deg, 0)$

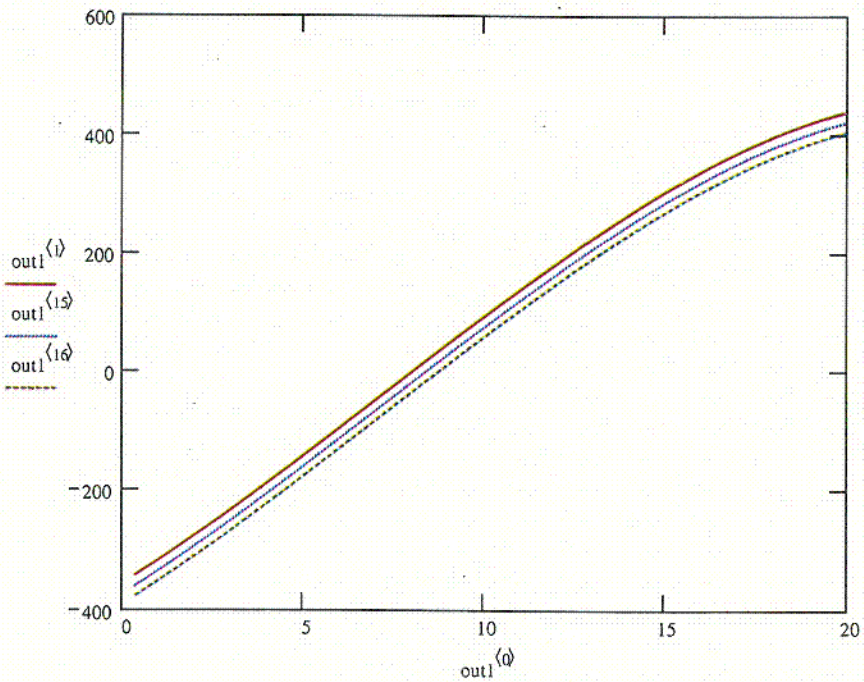

$out1^{\langle 17 \rangle} := K_{u1}(90 \cdot deg, 0)$ $out1^{\langle 18 \rangle} := K_{u1}(180 \cdot deg, 0)$

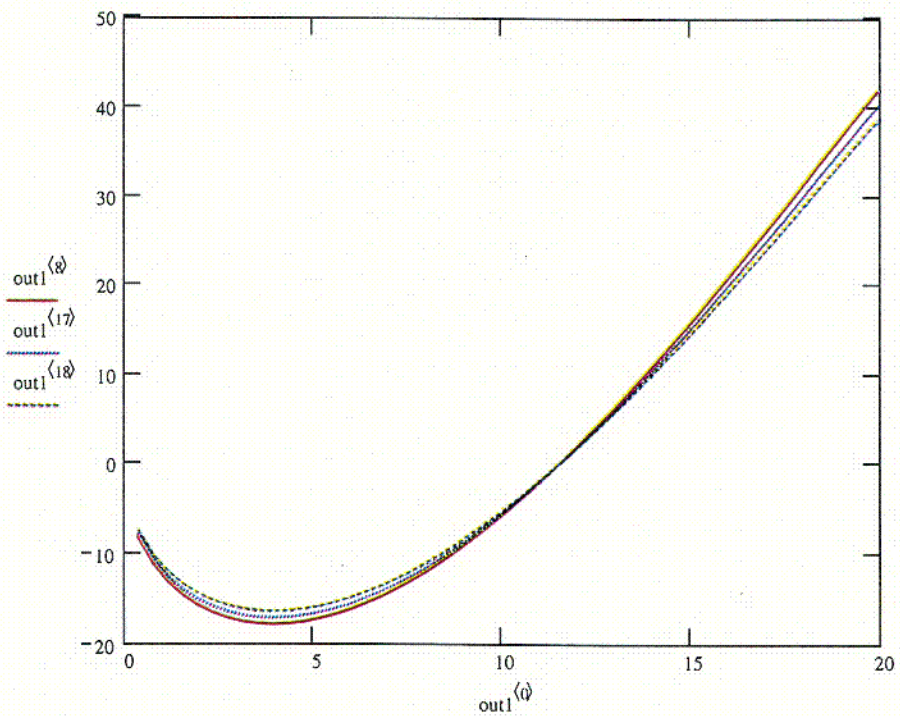

C14

Uncertainty Model 2:- Variation with z

$$s_{u2}(\theta, z) := \overrightarrow{s(x, \theta)} + sz(z)$$

$$K_{u2}(\theta, F) := K \cdot \frac{s(xf, \theta)}{s(xf, 0.0)} + sz(F) \cdot 0.058534 \cdot \sqrt{\pi \cdot x}$$

$out2^{\langle 0 \rangle} := depth$

$out2^{\langle 1 \rangle} := s_{u2}(0, 0)$

$out2^{\langle 2 \rangle} := s_{u2}(0, 0.5)$

$out2^{\langle 3 \rangle} := s_{u2}(0, -0.5)$

$out2^{\langle 4 \rangle} := s_{u2}(0, 1)$

$out2^{\langle 5 \rangle} := s_{u2}(0, -1)$

$out2^{\langle 6 \rangle} := s_{u2}(0, 3)$

$out2^{\langle 7 \rangle} := s_{u2}(0, -3)$

Stresses evaluated at various values of z, i.e., z = ± 0.5, ± 1, and ± 3 at θ = 0°.

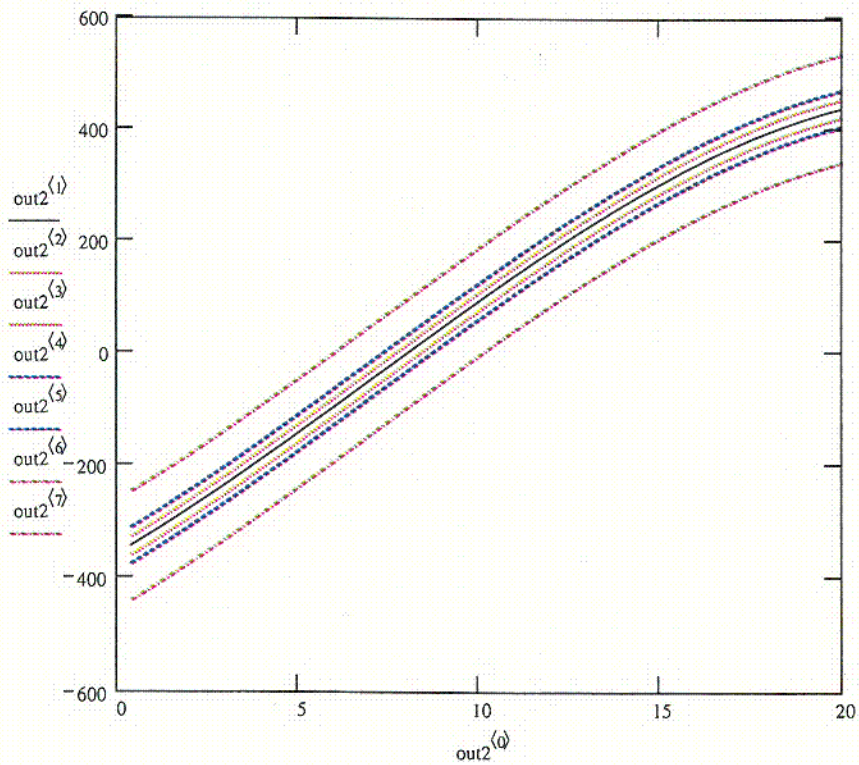

C15

$out2^{\langle 8 \rangle} := K_{u2}(0, 0)$ $out2^{\langle 12 \rangle} := K_{u2}(0, -1)$

$out2^{\langle 9 \rangle} := K_{u2}(0, 0.5)$ $out2^{\langle 13 \rangle} := K_{u2}(0, 3)$

$out2^{\langle 10 \rangle} := K_{u2}(0, -0.5)$ $out2^{\langle 14 \rangle} := K_{u2}(0, -3)$

$out2^{\langle 11 \rangle} := K_{u2}(0, 1)$

Stress Intensity Factor Profile evaluated at various values of z, i.e.,
$z = \pm 0.5, \pm 1$, and ± 3 at $\theta = 0°$.

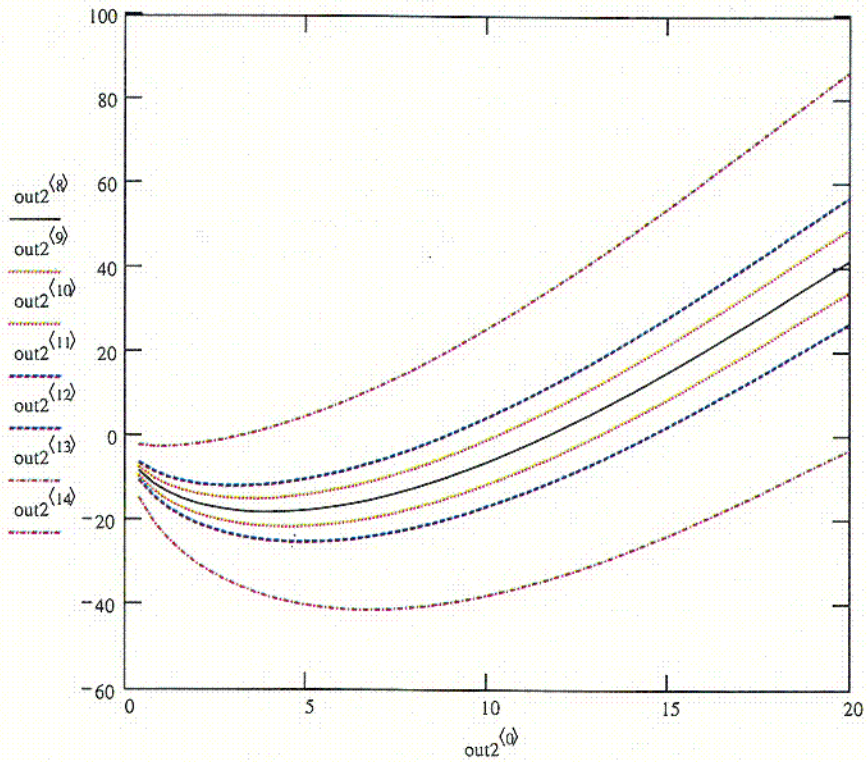

C16

Attachment III

Uncertainty and Variability Models - Flat Closure Lid

Input values:

$$a := \begin{pmatrix} -437.720543 \\ 176.967239 \\ -15.606072 \\ 0.367099 \end{pmatrix}$$ Stress Coefficients

$YS := 322.3$ Yield Strength in MPa

$Ktable :=$

-7.201806	0.3277
-10.051172	0.6579
-12.146611	0.9855
-13.83718	1.3132
-15.260512	1.6408
-16.488139	1.971
-17.608739	2.2987
-18.62418	2.6264
-19.34568	2.954
-18.273539	3.2842
-17.058768	3.6119
-15.735432	3.9395
-14.406931	4.2697
-13.095022	4.5974
-11.744104	4.9251
-10.371298	5.2527
-8.992063	5.5829
-7.6199597	5.9106
-6.283492	6.2382
-5.0215477	6.5659
-3.7917666	6.8961
-2.6026426	7.2238
-1.4618568	7.5514
-0.3762625	7.8791
0.6479086	8.2093
1.6027394	8.5369
2.4898903	8.8646
3.3047044	9.1948
4.043028	9.5225
4.7012569	9.8501
5.2762265	10.1778
5.8092533	10.508
6.2674598	10.8356
6.6339899	11.1633
6.9072392	11.491
7.0861418	11.8212
7.1700165	12.1488
7.1717966	12.4765
7.082153	12.8067
6.8851964	13.1343
6.581696	13.462
6.1730143	13.7897
5.6610523	14.1199
5.214087	14.4475
5.185517	14.7752
5.0926208	15.1028
4.9406399	15.433
4.7352551	15.7607
4.482741	16.0884
4.1899543	16.4186

$K := Ktable^{\langle 0 \rangle}$

$x := Ktable^{\langle 1 \rangle}$

This is the stress intensity factor (MPa m½) (column 0) versus depth (mm) (column 1).

$F := 0.3$ The maximum fraction of yield stress

$sz(z) := \frac{z \cdot YS \cdot F}{3}$ The uncertainty scaling factor.
z = ± 0.5 yields the ± 5% bounds
z = ± 1.0 yields the ± 10% bounds
z = ± 3.0 yields the ± 30% bounds

$$s(x,\theta) := \left[a_0 + x\cdot\left[a_1 + x\cdot\left(a_2 + x\cdot a_3\right)\right]\right] - (2.5\cdot 6.894757)\cdot(1 - \cos(\theta))$$

Stress as a function of depth, x, and angle, θ.

$sinf := 0.60887312121$ Angular correction for crack growth path

$depth := x\cdot sinf$

$xf := x_{last(x)}$ The last entry in the stress intensity factor table is considered the total thickness for this calculation since this is the largest thickness for which data is available.

Uncertainty Model 1 - Variation with z

$$s_{u1}(\theta,z) := \overrightarrow{s(x,\theta)}\cdot\left(\frac{s(xf,\theta) + sz(z)}{s(xf,\theta)}\right)$$

Stress

$$K_{u1}(\theta,z) := K\cdot\frac{s(xf,\theta) + sz(z)}{s(xf,0)}$$

Stress Intensity Factor

$out1^{\langle 0\rangle} := depth$

$out1^{\langle 1\rangle} := s_{u1}(0,0)$

$out1^{\langle 2\rangle} := s_{u1}(0,0.5)$

$out1^{\langle 3\rangle} := s_{u1}(0,-0.5)$

$out1^{\langle 4\rangle} := s_{u1}(0,1)$

$out1^{\langle 5\rangle} := s_{u1}(0,-1)$

$out1^{\langle 6\rangle} := s_{u1}(0,3)$

$out1^{\langle 7\rangle} := s_{u1}(0,-3)$

Stresses evaluated at various values of z, i.e., z = ± 0.5, ± 1, and ± 3 at θ = 0°.

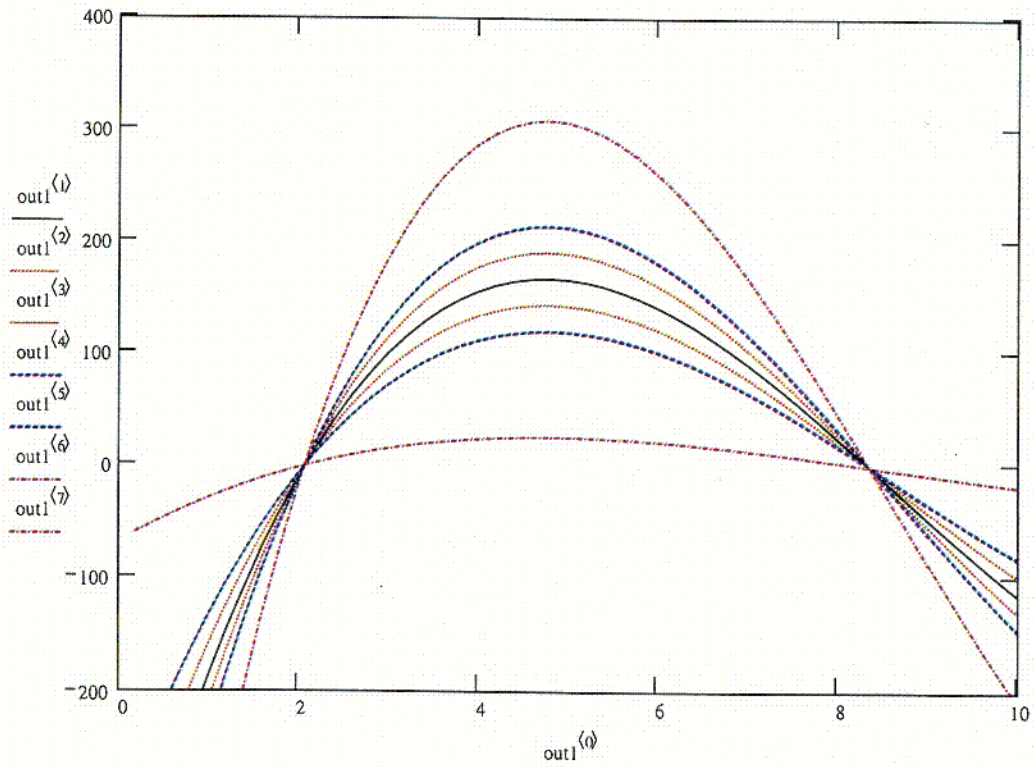

C17

$out1^{\langle 8 \rangle} := K_{u1}(0,0)$

$out1^{\langle 9 \rangle} := K_{u1}(0,0.5)$

$out1^{\langle 10 \rangle} := K_{u1}(0,-0.5)$

$out1^{\langle 11 \rangle} := K_{u1}(0,1)$

$out1^{\langle 12 \rangle} := K_{u1}(0,-1)$

$out1^{\langle 13 \rangle} := K_{u1}(0,3)$

$out1^{\langle 14 \rangle} := K_{u1}(0,-3)$

Stress Intensity Factors evaluated at various values of z, i.e.,
z = ± 0.5, ± 1, and ± 3 at θ = 0°.

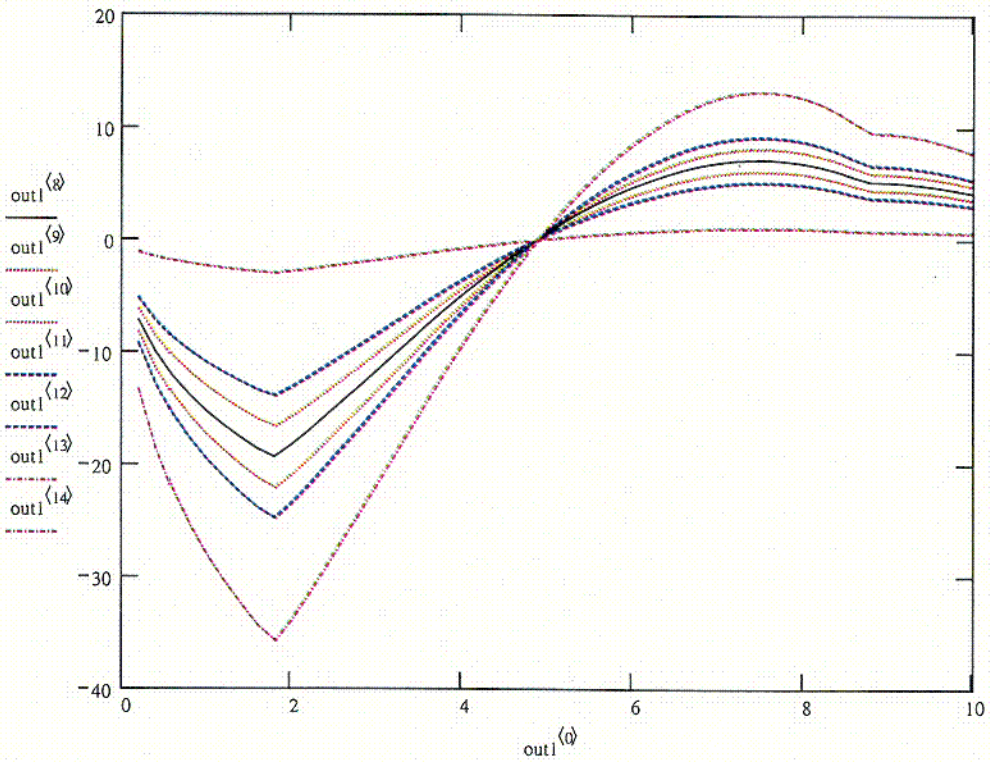

C18

Uncertainty Model 1 - Variation with angle, θ

$out1^{\langle 15 \rangle} := s_{u1}(90 \cdot deg, 0)$ $out1^{\langle 16 \rangle} := s_{u1}(180 \cdot deg, 0)$

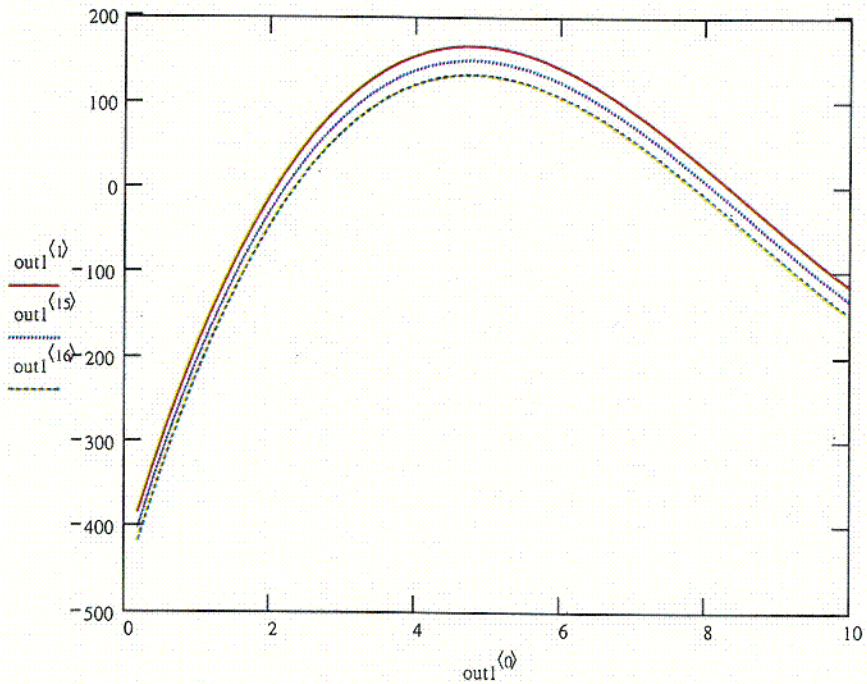

$out1^{\langle 17 \rangle} := K_{u1}(90 \cdot deg, 0)$ $out1^{\langle 18 \rangle} := K_{u1}(180 \cdot deg, 0)$

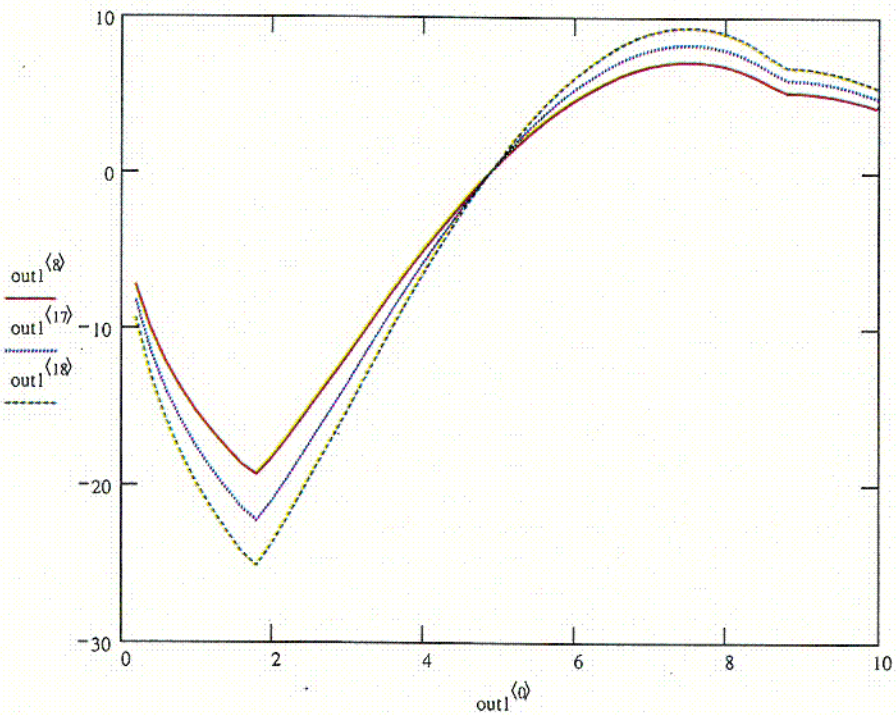

Uncertainty Model 2:- Variation with z

$$s_{u2}(\theta, z) := \overrightarrow{s(x, \theta)} + sz(z)$$

$$K_{u2}(\theta, z) := K \cdot \frac{s(xf, \theta)}{s(xf, 0.0)} + sz(z) \cdot 0.058534 \cdot \sqrt{\pi \cdot x}$$

$out2^{\langle 0 \rangle} := depth$

$out2^{\langle 1 \rangle} := s_{u2}(0, 0)$

$out2^{\langle 2 \rangle} := s_{u2}(0, 0.5)$

$out2^{\langle 3 \rangle} := s_{u2}(0, -0.5)$

$out2^{\langle 4 \rangle} := s_{u2}(0, 1)$

$out2^{\langle 5 \rangle} := s_{u2}(0, -1)$

$out2^{\langle 6 \rangle} := s_{u2}(0, 3)$

$out2^{\langle 7 \rangle} := s_{u2}(0, -3)$

Stresses evaluated at various values of z, i.e., z = ± 0.5, ± 1, and ± 3 at θ = 0°.

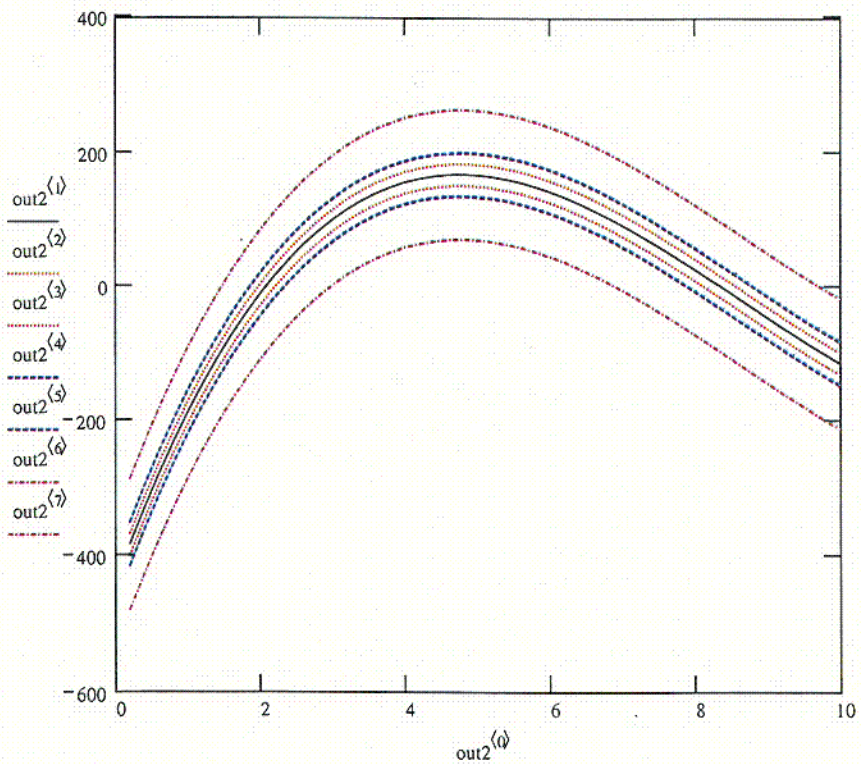

C20

$out2^{\langle 8 \rangle} := K_{u2}(0, 0)$

$out2^{\langle 9 \rangle} := K_{u2}(0, 0.5)$

$out2^{\langle 10 \rangle} := K_{u2}(0, -0.5)$

$out2^{\langle 11 \rangle} := K_{u2}(0, 1)$

$out2^{\langle 12 \rangle} := K_{u2}(0, -1)$

$out2^{\langle 13 \rangle} := K_{u2}(0, 3)$

$out2^{\langle 14 \rangle} := K_{u2}(0, -3)$

Stress Intensity Factor Profile evaluated at various values of z, i.e.,
z = ± 0.5, ± 1, and ± 3 at θ = 0°.

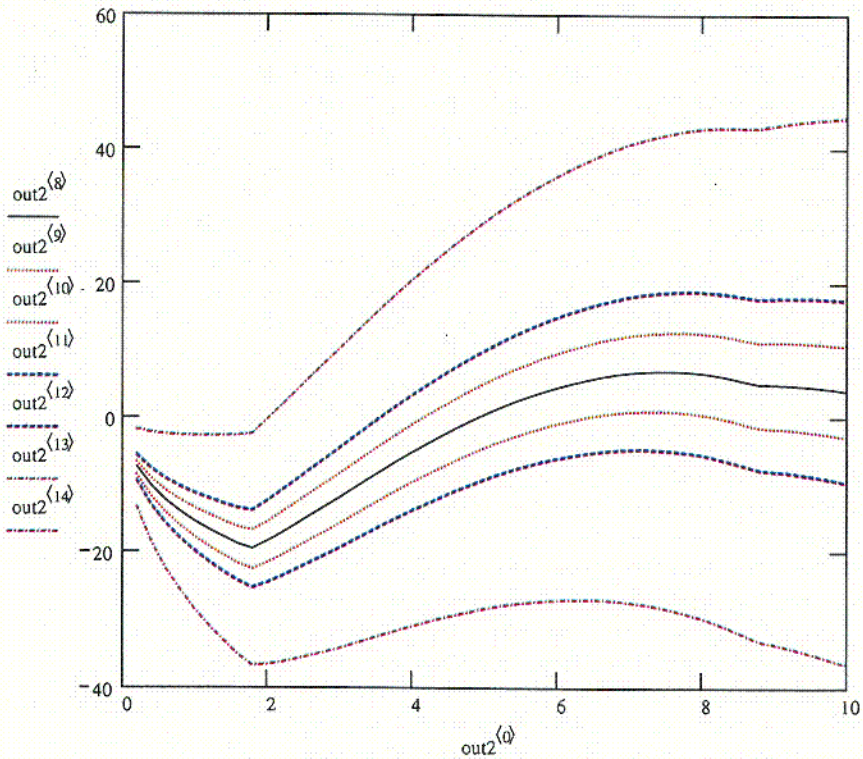

C21